QoS in Distributed Broadband Wireless Communication (BWC) Systems with Optimum Antenna Layout

Yao Yao

A Thesis

in

The Department

of

Electrical and Computer Engineering

Presented in Partial Fulfillment of the Requirements

for the Degree of Master of Applied Science

(Electrical and Computer Engineering) at

Concordia University

Montreal, Quebec, Canada

April 2012

CONCORDIA UNIVERSITY
SCHOOL OF GRADUATE STUDIES

This is to certify that the thesis prepared

By: Yao Yao

Entitled: "QoS in Distributed Broadband Wireless Communication (BWC) Systems with Optimum Antenna Layout"

and submitted in partial fulfillment of the requirements for the degree of

Master of Applied Science

Complies with the regulations of this University and meets the accepted standards with respect to originality and quality.

Signed by the final examining committee:

_____ Chair
Dr. R. Raut

_____ Examiner, External
Dr. C. Assi (CIISE) To the Program

_____ Examiner
Dr. W. Hamouda

_____ Supervisor
Dr. M. Mehmet-Ali

Approved by: _____
Dr. W. E. Lynch, Chair
Department of Electrical and Computer Engineering

_____20_____ _____
Dr. Robin A. L. Drew
Dean, Faculty of Engineering and
Computer Science

Abstract

QoS in Distributed Broadband Wireless Communication (BWC) Systems with Optimum Antenna Layout

Yao Yao

This thesis is concerned with optimization of distributed broadband wireless communication (BWC) systems. Distributed BWC systems contain a distributed antenna system (DAS) connected to a base station with optical fiber. Distributed BWC systems have been proposed as a solution to the transmit power problem in traditional cellular networks. So far, the research on BWC systems have advanced on two separate tracks, design of the system to meet the quality of service requirements (QoS) and optimization of layout of the DAS. This thesis considers a combined optimization of BWC systems. We consider uplink communications with multiple levels of priority traffic having any renewal arrival and departure processes. We develop an analysis that determines packet delay violation probability for each priority level as a function of the outage probability of the distributed antenna system. Then, we determine the optimal locations of the antennas that minimize the antenna outage probability, taking path-loss model, Rayleigh model and inter-cell interferences into account. We also study the tradeoff between the packet delay violation probability and packet loss probability.

ACKNOWLEDGEMENTS

I'd like to give my sincere gratitude to my supervisor Professor Mustafa Mehmet-Ali, for his patient guidance and the valuable suggestions he gave me when I faced with problems out of my league. He has always been able to spend time on my research problems no matter how busy he was. Furthermore, I'd say I have been deeply influenced by his conscientiousness, insightfulness and patience. For me, it is a very precious experience working with him. And I'd like to thank him again for this.

I'd like to express appreciations to my parents for their consistent supports and care.

Also I'd like to thank my friends for the accompanying in these two years.

Contents

List of Figures

List of Tables

List of Symbols

A. Symbols in Chapter 2

$A(t)$	The number of packet arrivals during time interval [0, t)
$A^V(t)$	The number of voice packet arrivals during interval [0, t).
$A^{D_1}(t)$	The number of D_1 packet arrivals during interval [0, t).
$A^{D_2}(t)$	The number of D_1 packet arrivals during interval [0, t).
$C(t)$	The number of departures during the interval [0, t)
$C^{D_1}(t)$	The number of D_1 packets that may be served during interval [0, t) in a queue with only D_1 traffic
$C^{D_1}{}'(t)$	The number of D_1 packets that may be served during interval [0, t) in a queue with the presence of voice traffic
$C^{D_2}(t)$	The maximum number of D_2 packets that may be served during [0, t) if there is no other traffic involved
$C^{D_2}{}'(t)$	The maximum number of D_2 packets that may be served during [0, t) in the presence of voice traffic and D_1 traffic
D	The queuing delay
D_{th}	The queuing delay threshold

k_i i from 0 to $A^{D_1}(t)$, for all the D_1 packets arrives during [0, t), each of them will cost k_i slots before transmitted successfully or dropped

L The maximum number of transmission tries of a D_1 packet

$M_C^{D_1}(z)$ The PGF of the service time of a single D_1 packet which has a truncated geometric distribution

$Prob(packet\ loss)$: The packet loss probability

p The system's average outage probability, it has the same meaning as $E(\mathbb{P})$

$\Lambda_A(\theta)$ The energy function of an arrival process

$\Lambda_A^{D_1}(\theta)$ The energy function of $A^{D_1}(t)$

$\Lambda_A^{D_2}(\theta)$ The energy function of $A^{D_2}(t)$

$\Lambda_C(\theta)$ The energy function of a saturated departure process

$\Lambda_C^{D_1}(\theta)$ The energy function of $C^{D_1}(t)$

$\Lambda_C^{D_1'}(\theta)$ The energy function of $C^{D_1'}(t)$

$\Lambda_C^{D_2}(\varphi)$ The energy function of $C^{D_2}(t)$

$\Lambda_C^{D_2'}(\varphi)$ The energy function of $C^{D_2'}(t)$

λ_V The arrival rate of Poisson arrival process of voice flow

λ_{D_1} The arrival rate of Poisson arrival process of D_1 flow

λ_{D_2} The arrival rate of Poisson arrival process of D_2 flow

μ, σ^2 The mean and variance of the service time of a single D_1 packet

$\mu_{D_2}, {\sigma_{D_2}}^2$ The mean and variance of the service time of a single D_2 packet

B. Symbols in Chapter 3

$E(\mathbb{P})$	The average or expected outage probability for the system
F	The cluster size of the cellular network with value of 7 in this thesis
$\hbar$	The height of the antennas
$h_{m,i}$	The identical independent distributed (i.i.d) complex Gaussian random variable (rv) representing Rayleigh fading between user in cell i to antenna m in the target cell
K	Equals to $(2^R - 1)$
M	The amount of antennas in a cell
$\mathbb{P}(outage)$	The outage probability for the system given a specific neighboring user locations set $(\boldsymbol{\ell}, \boldsymbol{\theta}, \mathbf{0})$
$P_m(outage)$	The outage probability for a single antenna m given a specific neighboring user locations set $(\boldsymbol{\ell}, \boldsymbol{\theta}, \mathbf{0})$
r	The radius of a cell
R	The required transmission rate or spectrum efficiency in bits/sec/Hz
$S_{m,i}$	The received signal strength at the antenna m from user i
W	The unitary signal strength
η	The path loss exponent
$\rho_{m,i}$	The distance from user i to the antennas m in the target cell
Γ_m	The instantaneous SNR at the antenna m in the target cell
$(\ell_i, \theta_i, 0)$	Polar Coordinate of user i wrt to the center of the cell A_i,
$(L_m, \Theta_m, \hbar)$	Polar Coordinate of antenna m wrt to the center of cell A_0,
$(L'_M, \Theta'_M, \hbar)$	Polar Coordinate of optimum location of antenna m wrt to the center of A_0

$(\boldsymbol{\ell}, \boldsymbol{\theta}, \mathbf{0})$ The user locations vector, $(\boldsymbol{\ell}, \boldsymbol{\theta}, \mathbf{0}) = \{(\ell_0, \theta_0, 0), (\ell_1, \theta_1, 0), \dots, (\ell_{F-1}, \theta_{F-1}, 0)\}$

$\boldsymbol{L}$ The antennas location vector, $\boldsymbol{L} = [(L_1, \Theta_1, \hbar), \dots, (L_M, \Theta_M, \hbar)]$

$\boldsymbol{L}'$ The optimum antennas location vector, $\boldsymbol{L}' = [(L'_1, \Theta'_1, \hbar), \dots, (L'_M, \Theta'_M, \hbar)]$

$(x_i, y_i, 0)$ Cartesian coordinate of user *i* with respect to (wrt) the center of cell A_0.

$(x_i, y_i, 0) = \left(x_i^C + \ell_i \cos\theta_i, y_i^C + \ell_i \sin\theta_i, 0\right)$

$(X_m, Y_m, \hbar)$ Cartesian coordinate of antenna *m* wrt the center of cell A_0.

$(X_m, Y_m, \hbar) = (L_m \cos(\Theta_m), L_m sin(\Theta_m), \hbar)$

$(x_i^C, y_i^C, 0)$ Cartesian coordinate of cell A_i's center wrt the center of the target cell A_0.

Chapter 1. Introduction

1.1 Quality of Service (QoS) of a distributed broadband wireless communications (BWC) system

The fast development of wireless networks requires higher transmission rates. The required access rate is increasing up to 1Gbits/s for the next generation (4G) communication systems according to the objective of IMT-Advanced (International Mobile Telecommunications) system, which is set by ITU-R (International Telecommunication Union- Radiocommunication Standardization Sector) [1][2][3]. However, the constraint on the transmit power limits the transmission rate, especially for mobile users having power and energy constraints, such as smart phones and pads. One promising way to solve this problem is the distributed broadband wireless communications (BWC) systems [2].

A distributed BWC system is made up of a distributed antenna system (DAS) and radio over fiber (RoF) technology [2]. The idea of DAS is that rather than having antenna(s) set at the center of a cell, which is called centralized antenna system (CAS),

the antennas are located geographically separately in the cell [2]. The RoF technology, which is very reliable and has very small delay, is responsible for the transmission between these antennas and a central processor where they are jointly processed [2]. In this way, a user is very likely to have an antenna nearby comparing to a CAS, it will in turn reduce the transmission power requirement of that user and also the antennas. What's more, the distributed antennas are usually cheaper so it's possible to place many distributed antennas in one cell [6].

The distributed BWC system solves the power constraint problem very well instead of shrinking the cell size as in conventional CAS, which results in larger overhead and delay due to higher frequency of handovers between cells.

1.1.1 QoS criteria in DAS

Since RoF technology is very reliable and generates very small delay for communications, QoS requirements for distributed BWC systems are essentially the requirements for DAS.

Different traffic types may have different QoS requirements. For example, real time traffic such as voice and video always has strict requirements on delay and jitter. At the same time, they are usually redundant thus accuracy of the delivered information is not a critical QoS requirement. On the other hand, data traffic such as e-mail, file

transfers and distributions, are usually delay-insensitive but accuracy-sensitive thus their QoS mainly focus on packet loss or outage probability (an outage refers to a transmission that is not received successfully by the receiver side). There is also some traffic with intermediate QoS requirements in between the two extremes.

1.1.2 Review of previous work on DAS

Initially, the objective of DAS was to cover the dead spots at indoor situations while now it has been demonstrated to have the advantage of decreasing the transmission power and increasing the system capacity [4], [8], [9].

In [4], it has been shown that distributed antenna systems have better performance than centralized antenna systems. They demonstrated that the capacity of a centralized antenna array grows linearly with the number of antennas, and distributed antenna array system can offer an additional growth. This result is based on the assumption of dividing a cell into several microcells and placing an antenna at the center of each microcell. However, no justification is given for this placement of antennas.

In [8], they assume the randomly distributed antenna topology to prove that the mean spectral efficiency of DAS is higher than CAS, since in DAS the mean square access distance (MSAD) is less than that in a conventional CAS. Though this early paper

(in 2003) does not discuss the location of antennas, it gives the first clue that the locations of antenna matters a lot in performance.

In [9], the same randomly distributed layout is considered as in [8]. The work shows that DAS performs better than CAS in power efficiency which in turn, improves the system capacity. In [9], it is also shown that with the increase of the number of distributed antennas, the capacity gain is sharply increasing.

In [5], they study the uplink sum-rate capacity with per user power constraint in a single cell with multiple users and DAS with circular antenna layout. They give an iterative method for obtaining the closed form for the capacity. However, their work only works for a single cell with no inter-cell interferences involved and the radius of the antenna circle is chosen without justification.

As discussed above, most of the early work in DAS is concerned only with the advantages of DAS over CAS, with no attention has been paid to the optimum layout of DAS or the QoS in DAS. However, recently, some work started to appear on the optimum layout of DAS, based on different system performance metrics such as capacity, spectrum and power efficiencies, like in [6], [24], [25] and [10]. And some other work started to interested in quality of service requirements (QoS) in DAS such as delay and outage probability, like in [13] and [11].

As an extension of the work in [5], reference [6] aims to optimize the sum-rate uplink capacity of a single cell with multiple users by determining the optimal radius of the antenna circle with assumptions that the antennas are placed on a circle centered at the cell center and their locations on the circle are uniformly distributed independent of each other. They obtain the optimal radius of the antenna circle for a specific case that the path loss exponent equals to 4. This work is more appropriate to a CDMA type of system since all the users in the cell will be transmitting simultaneously. Inter-cell interferences are not considered in this thesis.

In [24], they aim to maximize the cell averaged uplink ergodic capacity by converting the optimization location problem into a codebook design problem, and the squared distance criterion is proposed to simplify it through a series of approximations. To simplify their work, they assume a circular antenna layout and then they determine the optimal antenna layout for the uniformly distributed users' case analytically and for the generalized distributed users' case numerically. Their work is also based on a single cell uplink model and the interference from other cells is not considered. [25] is a very similar work which studies the downlink communications with selective transmission.

In [10], the optimal location of antennas in a cellular setting has been studied for the downlink communications based on the performance metrics of capacity and power efficiency, taking inter-cell interferences into account with log-normal shadowing and

Rayleigh fading channel models. Their work uses the Robbins-Monro procedure from stochastic approximation theory to determine the best location of antennas through a simple numerical method. Though no closed form results are obtained, their results show that for a 7 antenna case, the optimal layout consists of placement of one antenna at the center and remaining ones on a circle around it without presenting the exact position of antennas on the circle, and they also determine that the size of the circle shrinks as the interference coefficient increases. They demonstrate that the optimal placement can provide reduction in power consumption, or it can increase the area spectral efficiency in some certain cases. They conclude from simulation results that shadowing or multi-path Raleigh fading has no effect on the optimal location of antennas, which is a really interesting conclusion, however, without mathematical proof.

For other works which concerned the QoS in DAS, most of them are interested in the problem of antenna selection and coordination in order to satisfy certain QoS requirements. For example, [13] is a work based on a distributed BWC system assuming that the central server maintains a separate queue for each of the users. This work considers selection of a subset of the available distributed antennas such that the probability of queuing delay (delay-bound violation probability) for users in the downlink transmission is less than a threshold.

[11] studies the impact of the size of base station clusters on decoding outage

probability in a distributed BWC system. It considers the effects of limited backhaul bandwidth and the size of overhead among cooperating base stations, in selecting an appropriate base station cluster to perform message decoding, since more base stations will cause more interactions thus more overhead and bandwidth will be required for the communications among them. This work employs different multi-cell processing (MCP) schemes: joint decoding versus local decoding; and different repeat-request mechanisms: Automatic Repeat-reQuest (ARQ) or Hybrid Automatic Repeat-reQuest (HARQ) in selecting base station cluster.

Our thesis will combined the above two tracks together, the optimization of antenna layout and QoS requirement, which to my knowledge, hardly any research has been done on these two aspects jointly.

1.1.3 Motivation for the thesis

For the next-generation communication system, the proportion of multi-media communications will increase continuously, and these different types of multi-media traffic are usually assigned different priorities to satisfy their QoS requirements such as delay. Thus, it is important to study the delay attribute in a general multi-priority queue, while former work on determining the queuing delay or the relating queuing length are

mostly based on a single type of traffic with specific arrival/departure such as Poisson process and constant process, like in [13][22][23].

Also as can be seen from the above introduction, distributed BWC system is a very promising technology and the location of the distributed antennas is a vital issue in it. That's why we base our work on a distributed BWC and try to find the optimum antenna layout. Also, we consider uplink communications since we believe it is more crucial on the aspect of the power constraint problem of users. Furthermore, we take co-channel interferences into account since its more real while most of the work on optimization of antenna layout only consider a single cell with no co-channel interferences, such as [5][6][24], as was introduced in section 1.1.2.

1.1.4 Problem statement

In this thesis, we consider a cross-layer work combining the QoS in DAS and the optimization of distributed antenna layout together.

At Mac layer, we consider uplink communications, from user to base station, with multiple levels of priority traffic, having any renewal arrival/departure processes. We determine one QoS criterion, the packet delay violation probability, for each priority level as a function of the outage probability of the distributed antenna system. We also

study the tradeoff between the packet delay violation probability and packet loss probability.

Then at Physical layer, we determine the optimal antenna layout that minimizes the average uplink outage probability of DAS. Fadings and co-channel interferences are taken into account in our analysis.

1.2 Background knowledge

Next, we describe the background knowledge needed for this thesis.

1.2.1 Cellular networks

In cellular networks a geographical area is divided into several cells with each having a base station usually located at the center of the cell. The shapes of these cells are assumed to be hexagonal or circle and their sizes depend on the density of the users, the capacity of the base station and available frequency bandwidth. A base station serves to the users in its own cell. Communication between different base stations enables the user to communicate with users in different cells. A typical cellular network topology is shown in Figure 1.1.

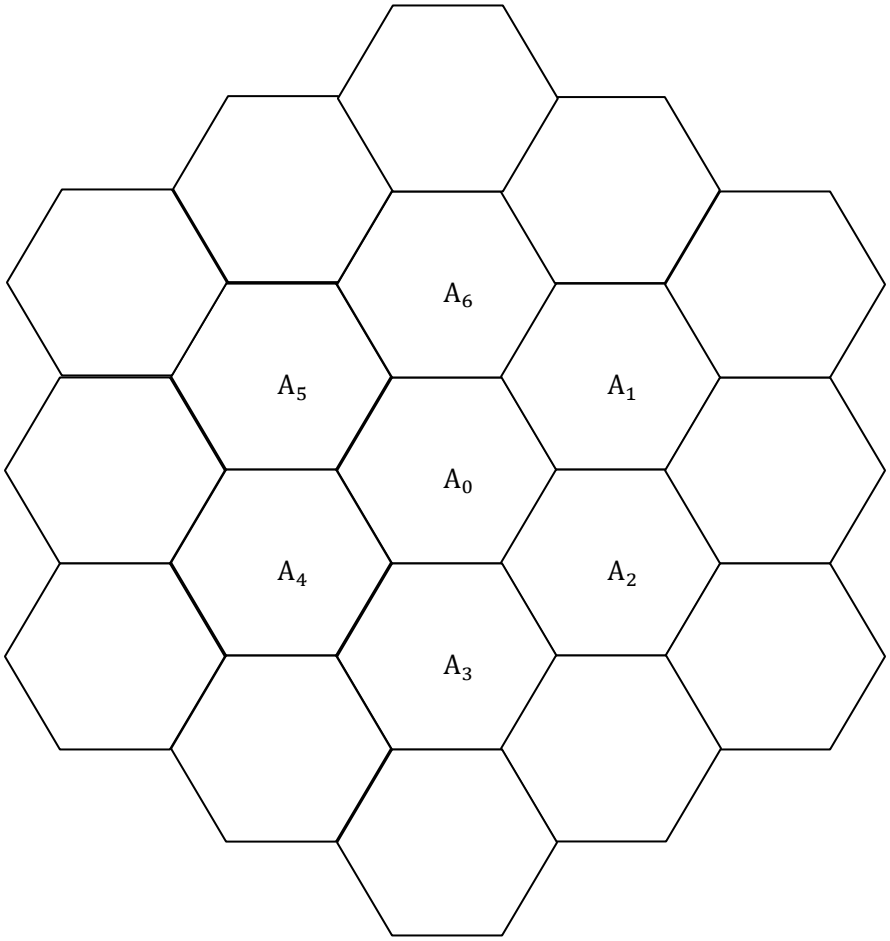

Figure 1.1: Typical cellular network topology

As may be seen, the area is divided into hexagonal cells with each cell having six tier-one neighbors and 12 tier-two neighbors. Since communications between base stations and users are wireless, there might be a lot of interference between the cells. One solution to this problem is not to allow a cell to use the same frequency band as any of its tier-one neighbors. This forms a cluster of 7 cells, each of these 7 cells using a different frequency band. The frequency reuse factor for such a cluster is 1/7 since each cell uses 1/7 of all the available bandwidth. As in Figure 1.1, each of the cells in the central cluster

are using a different 1/7 of total bandwidth to avoid interference among each other. Same thing is in every cluster of 7 cells.

When a user moves from one cell to another during a call, handover is implemented between the two base stations serving to these cells which causes overheads.

1.2.2 Probability of outage

Outage probability is a very common and important metric for QoS in wireless networks. Since wireless environments are time-varying due to relative motions between transmitter-receiver pair and changes of environment between it, etc, the channel capacity can be very unstable in the time domain. When the instantaneous channel capacity drops below a certain threshold, a channel outage will happen which will cause packet losses. This may be a severe problem in large number for applications [17].

1.2.3 ARQ mechanism

One possible method to allay the impact of outage is to use Automatic Repeat Request (ARQ) retransmission mechanism. This mechanism mitigates packet losses but at the expense of higher bandwidth consumption and larger queuing delay. This is explained

below. The probability of packet loss may be determined by,

$$Prob(packet\ loss) = p^L$$

where p denotes the outage probability and L denotes the maximum number of allowed transmissions of a packet assuming each transmission is independent. On the other hand, reduction of L can reduce the delay but as mentioned before, it may not be a good mechanism for accuracy-sensitive traffic since it will raise more packet losses. So there is a tradeoff between packet loss probability and delay, in adjusting L.

1.2.4 Local decoding versus joint decoding

With local decoding in the uplink, each antenna in the same cell will decode the received packets from users and send their decoding results to the central processor. Only one successful decoding result is enough for the central processor to obtain packet correctly. So when a central processor cannot get the correct information, it means that none of the antennas has been able to decode the packet successfully.

With joint decoding, each antenna transmits the received soft information to the central processor which does decoding. In this scenario, the antennas function like relays and pass the information to the central processor, and then the central processor will multiplex all the information based on specific mechanisms and perform decoding of the

merged signal. In this case, decoding only takes place at the central processor, and antennas can simply be treated as relays.

In our work, we only consider local decoding.

1.2.5 Multi-priority queue

For the next generation communication networks, multimedia services will make a large portion of a user's traffic including voice, e-mail, messaging, files transfers and distribution services [27]. Thus the service queue of a user is very likely to contain packets from multiple classes of traffic with different Quality of Service (QoS) requirements. Those multiple classes of traffic may be assigned different priorities according to their own QoS requirements. Those low priority traffic will be transparent to the high priority traffic and can be transmitted only if there is no pending packet with higher priority.

1.3 Outline

In the following, outline of the thesis is presented.

In Chapter 2, we consider uplink communications with multiple levels of priority traffic. We develop an analysis that determines packet delay violation probability for each

priority level as a function of the outage probability. In section 2.1, we present the queuing model. In section 2.2, we determine the queuing delay violation probability for a sole data traffic flow and then extend the results to a dual-priority queue in 2.2.1 and 2.2.2 respectively. And in 2.2.3, we demonstrate that the analysis can be easily extended to a multi-priority queue with any number of priority levels and any traffic arrival/departure processes as long as they are renewal processes. Then in section 2.3, we give numerical results for the analysis of the dual-priority queue, we also show the tradeoff between the packet delay violation probability and packet loss probability. Simulation results are also presented in section 2.4.

From the work in Chapter 2 we learn that the reduction of outage probability improves the system's QoS and performance in several ways. So in Chapter 3, we study the optimum antenna layout in DAS that minimizes the outage probability of the system. The system model of DAS is described in section 3.1, and then we determine the outage probability for a single antenna in section 3.2 through application of Laplace transform techniques. After that, we obtain the average or expected outage probability for the system in section 3.3 and the expression of the optimal location of antennas in section 3.4. Due to mathematic difficulties, we could not determine the closed form expression for the optimal locations of antennas. The numerical and simulation results are presented in section 3.5 and 3.6 respectively instead.

Finally, Chapter 4 presents the conclusions of the thesis and the future work.

Chapter 2. Uplink queuing delay in a multi-priority queue under heavy traffic load

When designing a system, queuing delay is always a crucial quality of service (QoS) metric. Especially in a multi-priority queue, the delay of the low priority traffic may be very large when the queue is under heavy load, and some QoS requirements maybe violated if the delay exceeds a set threshold value. Furthermore, if we consider retransmission mechanisms due to outages caused by the instability of wireless environment, this situation may be even worse. So in this chapter, we will study the uplink queuing delay violation probability in a multi-priority queue under heavy traffic load, as a function of the outage probability of the system.

We assume that each user may generate a delay-sensitive and a relatively insensitive flow, let's say a voice flow and a data flow D_1, respectively, and the voice flow will be given a higher priority than D_1. Based on this assumption, we will determine the queuing delay violation distribution of the D_1 traffic using approximate

methods, and numerical and simulation results will be presented after that. Though it is a dual-priority queue, the same analysis can easily be applied to multi-priority queues, which will be shown later.

2.1 Queuing model for uplink communications

In the section, we will present the queuing model for uplink communications, from the user to the base station.

We assume that both voice and D_1 packets arrive according to independent Poisson processes with rates λ_V and λ_{D_1} packets/sec respectively. The arriving packets are stored at the service queue with infinite buffer size. The time–axis is slotted and the transmission of a packet starts at the beginning of a slot, the duration of which equals to one slot.

We assume that the voice flow has higher priority than the data flow thus D_1 traffic will be transparent to the voice traffic and a D_1 packet will be transmitted at time *t* only if there is no pending voice packets at time t^-.

A transmitted packet may not be received successfully due to the poor channel condition, and this event will be treated as an outage. When outages occur, voice packets will not be allowed retransmission and will be dropped since voice is delay sensitive. D_1

packets, on the other hand, will be asked for retransmission and they will be dropped only if they could not be received successfully after L transmissions. Dropped D_1 packets will be treated as packet loss and probability of packet loss is given by,

$$Prob(packet\ loss) = p^L$$

where p is the outage probability and L stands for the maximum number of allowed transmissions of a D_1 packet. In this work, we do not consider the packet loss probability of voice packets since voice information is redundant and it can tolerate for packet losses.

2.2 Queuing delay for low priority traffic

Based on the queuing model described in the last section, D_1 packets may experience large delays because of buffering and retransmissions. So in this section, we are going to study the queuing delay violation probability for D_1 traffic.

We will first start by analyzing a simple case with only the D_1 traffic and no voice traffic in the system in section 2.2.1. Then in section 2.2.2, we will study the queuing delay violation probability of the D_1 traffic in the presence of voice traffic. After that, in section 2.2.3 we will extend the analysis to a system with three levels of traffic to demonstrate that our analysis applies to traffic with any number of levels.

Since in general it is unrealistic to determine the hard delay bound for a wireless system [13], we are going to employ the same metric as in [13], the queuing delay-bound violation probability, to study the queuing delay attribute of different flows. The queuing delay-bound violation probability is defined as the probability that the queuing delay exceeds a certain value, and it is defined as,

$$Prob(D > D_{th}) \qquad (2.1)$$

where D and D_{th} represent the queuing delay and a queuing delay threshold.

For a queue, let us define $A(t)$ as the number of source packet arrivals during time interval [0, t). Defining the energy function of that arrival process as $\Lambda_A(\varphi)$ [13],

$$\Lambda_A(\varphi) = lim_{t\to\infty} \frac{1}{t} log\, E\left(e^{\varphi A(t)}\right) \qquad (2.2)$$

Let us consider the departure process from the same queue assuming that this departure process is under saturation and independent of the arrival process [22]. Defining $C(t)$ as the number of departures during the interval [0, t) and $\Lambda_C(\varphi)$ as the corresponding energy function [22]:

$$\Lambda_C(\varphi) = lim_{t\to\infty} \frac{1}{t} log\, E\left(e^{\varphi C(t)}\right) \qquad (2.3)$$

From [13] and [22], we have the queuing delay-bound violation probability for a queue,

$$Prob(D > D_{th}) \approx e^{-\Lambda_A(\varphi^*)D_{th}} \tag{2.4}$$

where φ^* is the unique solution of $\Lambda_A(\varphi) + \Lambda_C(-\varphi) = 0$.

2.2.1 Delay violation probability of sole D_1 traffic

From (2.4), we can determine the queuing delay-bound violation probability of a queuing system if we know the energy function of the arrival and departure processes to/from that queue. So for the sole D_1 traffic, obtaining the energy functions of the D_1 packet arrival and departure processes are enough to determine the queuing delay-bound violation probability of it.

The energy function of a Poisson process has been determined in [21] and let $\Lambda_A^{D_1}(\varphi)$ denote the energy functions of the Poisson arrival processes of D_1 traffic, then, it is given by [21],

$$\Lambda_A^{D_1}(\varphi) = \lambda_{D_1}(e^{\varphi} - 1) \tag{2.5}$$

in $\Lambda_A^{D_1}(\varphi)$, the subscript A denotes the arrival process, and the superscript D_1 denotes D_1 traffic. This notation also applies to other energy functions.

Next, we will determine the energy function of the saturated departure process of D_1 traffic when there is no voice flow involved in the system. We will assume that the

consecutive transmissions of a packet are independent of each other and outage probability of each transmission is given by p. Then the service time k of each D_1 packet has truncated geometric distribution given by,

$$\begin{cases} Prob(k=i) = (1-p)p^{i-1} \; for \; i < L \\ Prob(k=i) = p^{L-1} \; for \; i = L \end{cases} \tag{2.6}$$

where the unit of k is in slots, L is the maximum number of transmissions of a D_1 packet and each transmission takes one slot.

Let $M_C^{D_1}(z)$ denote the probability generating function (PGF) of the above service time distribution, and substitute (2.6) in it, we have,

$$\begin{aligned} M_C^{D_1}(z) &= \sum_{i=1}^{\infty} z^i Prob(k=i) = \sum_{i=1}^{L-1} \left[z^i Prob(k=i) \right] + z^L Prob(k=L) \\ &= (1-p)z\frac{1-(zp)^{L-1}}{1-zp} + z^L p^{L-1} \end{aligned} \tag{2.7}$$

Then, the mean μ and variance σ^2 of the service time is given by,

$$\begin{cases} \mu = \left[M_C^{D_1}(z) \right]' \Big|_{z=1} = \frac{1-p^L}{1-p} \\ \sigma^2 = \left[M_C^{D_1}(z) \right]'' \Big|_{z=1} + \left[M_C^{D_1}(z) \right]' \Big|_{z=1} - \left\{ \left[M_C^{D_1}(z) \right]' \Big|_{z=1} \right\}^2 \\ \quad = \frac{-p^{2L} + p^{L+1}(-2L-1) + p^L(-2L+1) + 2p}{(1-p)^2} \end{cases} \tag{2.8}$$

Unfortunately, it is not possible to determine the energy function of this departure process. The inability to derive the energy function defined in (2.3) limits the

application of this approach to determine the delay violation probability of a packet in (2.4). This situation is common in obtaining the energy function since most processes may not have a closed form expression for energy function, even if there is a closed form, usually it is hard to obtain. In this work, we propose an alternative method to determine an asymptotic energy function, which will be applicable also to the other problems.

From the above analysis, we know that the intervals between consecutive departures which correspond to the service times as the queue is saturated, are independent identical distributed (i.i.d). Then we can model the departure process as a renewal process by taking the service time as the renewal interval, and the departure of a packet or the moment of completion a service as a renewal point. We propose to apply the central limit theorem for renewal processes [28], to determine $C^{D_1}(t)$, the distribution of the number of D_1 packets that may be served during [0, t). This theorem states that $C^{D_1}(t)$, asymptotically approaches to a Gaussian random variable as t goes to infinity, with mean $\frac{t}{\mu}$, and variance $\frac{\sigma^2 t}{\mu^3}$ where μ and σ^2 are the mean and variance of the renewal interval. Thus following (2.3), the energy function of the departure process of data traffic, $\Lambda_C^{D_1}(\varphi)$, is given by,

$$\Lambda_C^{D_1}(\varphi) = lim_{t\to\infty} \frac{1}{t} log\, E\left(e^{\varphi C^{D_1}(t)}\right) = lim_{t\to\infty} \frac{1}{t} log \left(e^{\frac{t\varphi}{\mu} + \frac{t\varphi^2\sigma^2}{2\mu^3}} \right) = \frac{\varphi}{\mu} + \frac{\varphi^2\sigma^2}{2\mu^3} \quad (2.9)$$

$E\left(e^{\varphi C^{D_1}(t)}\right)$ is the moment generating function of the Gaussian rv $C^{D_1}(t)$ with mean $\frac{t}{\mu}$,

and variance $\frac{\sigma^2 t}{\mu^3}$, so $E\left(e^{\varphi C^{D_1}(t)}\right) = e^{\frac{t\varphi}{\mu}+\frac{t\varphi^2\sigma^2}{2\mu^3}}$.

(2.9) is an asymptotic result of the energy function of the departure process of D_1 traffic when no voice traffic is involved. Subscript C in $\Lambda_C^{D_1}(\varphi)$ stands for the departure process.

Substituting (2.5), (2.9) into (2.4), then the delay violation probability of D_1 traffic is given by,

$$Prob(D > D_{th}) \approx e^{-\Lambda_A^{D_1}(\varphi^*)D_{th}}$$

where φ^* is the unique solution to of,

$$\Lambda_A^{D_1}(\varphi) + \Lambda_C^{D_1}(-\varphi) = 0$$

with

$$\begin{cases} \Lambda_A^{D_1}(\varphi) = \lambda_{D_1}(e^{\varphi} - 1) \\ \Lambda_C^{D_1}(\varphi) = \dfrac{\varphi}{\mu} + \dfrac{\varphi^2\sigma^2}{2\mu^3} \\ \mu = \dfrac{1-p^L}{1-p} \\ \sigma^2 = \dfrac{-p^{2L} + p^{L+1}(-2L-1) + p^L(-2L+1) + 2p}{(1-p)^2} \end{cases}$$

Now we are going to demonstrate that our asymptotic method from central limit theorem for renewal processes does provide very good approximation to the exact energy function with two examples, a Poisson process and a Binomial process, whose exact

energy functions are easily to obtain. The expressions of the asymptotic and exact energy functions of the above two processes are given below.

For a Poisson process with arrival rate λ_p, its exact energy function $\Lambda(\varphi)$ and the asymptotic energy function $\Lambda^{\wedge}(\varphi)$ when *t* goes to infinity are presented in [21],

$$\begin{cases} \Lambda(\varphi) = \lambda_p(e^{\varphi} - 1) \\ \Lambda^{\wedge}(\varphi) = \lambda_p\left(\varphi + \dfrac{\varphi^2}{2}\right) \end{cases}$$

and we notice $\Lambda^{\wedge}(\varphi)$ is a Taylor approximation of $\Lambda(\varphi)$ for Poisson processes.

For Binomial process with success probability 1-q, its exact energy function $\Lambda(\varphi)$ and the corresponding asymptotic energy function $\Lambda^{\wedge}(\varphi)$ are presented in [21],

$$\begin{cases} \Lambda(\varphi) = log(q + (1-q)e^{\varphi}) \\ \Lambda^{\wedge}(\varphi) = (1-q)\varphi + 1/2(1-q)q\varphi^2 \end{cases}$$

The asymptotic and the exact energy functions of Poisson and Binomial processes are plotted in Fig. 2.1as a function of φ. We can see that the asymptotic results are very close to the exact energy function for small values of φ. And for most stable queues under heavy loading, the φ^* satisfy (2.4) is far less than 1. Thus we can conclude that (2.9) is a good asymptotic result for the energy function of the departure process of D_1 traffic when no voice traffic is involved.

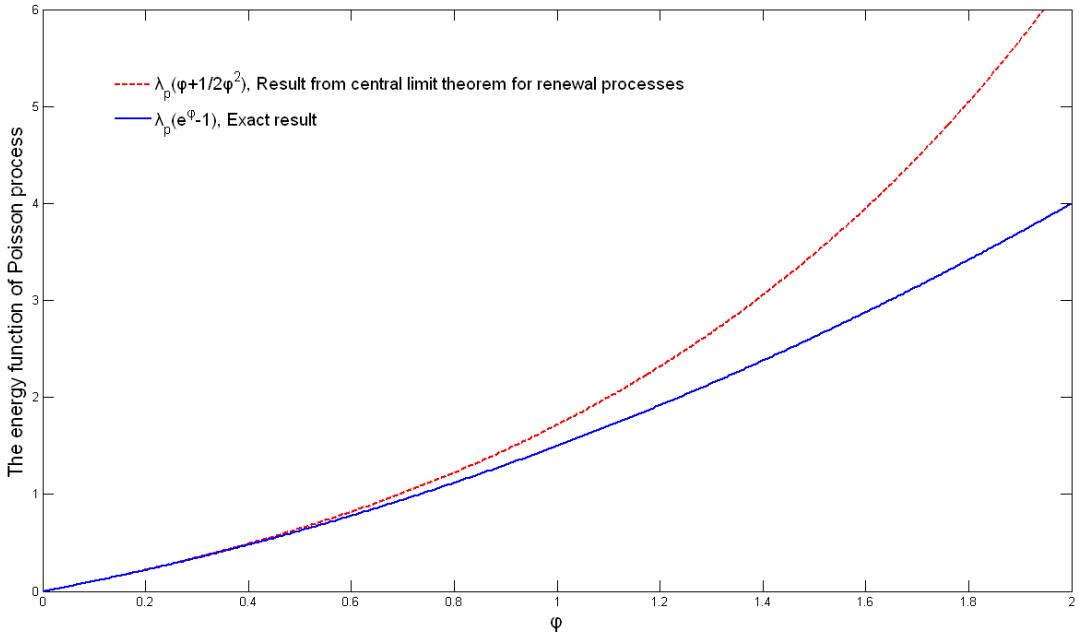

(a) Energy function of Poisson process with arrival rate λ_p

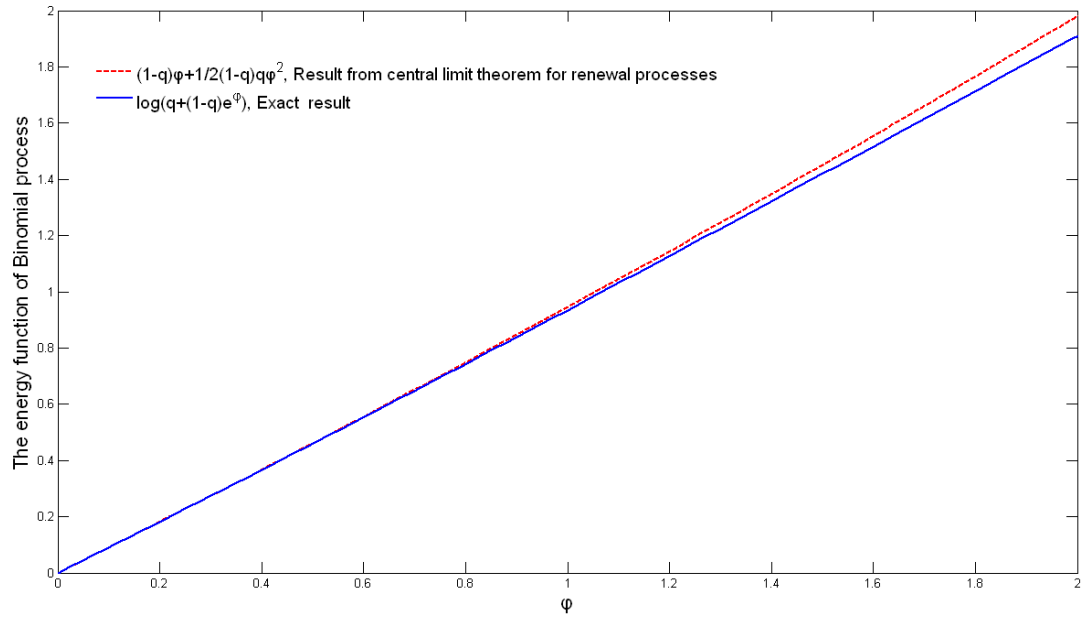

(b) Energy function of Binomial process with success probability 1-q

Fig. 2.1 Comparison of energy function from central limit theorem for renewal processes and the exact energy functions of Poisson and Binomial processes

2.2.2 Delay violation probability of D_1 traffic in the presence of voice traffic

Next, we consider transmission of D_1 packets in the presence of voice, which was described in the queuing model section. We let $\Lambda_A^{D_1'}(\varphi)$, $\Lambda_C^{D_1'}(\varphi)$ denote the energy functions of packet arrival and departure processes of D_1 traffic in the presence of voice. We notice that $\Lambda_A^{D_1'}(\varphi)$ remains the same as $\Lambda_A^{D_1}(\varphi)$ since arrival processes are independent. However, $\Lambda_C^{D_1'}(\varphi)$ differs from $\Lambda_C^{D_1}(\varphi)$, since voice has priority over D_1, D_1 traffic may only use the left over bandwidth from the voice traffic. Let $C^{D_1'}(t)$ denote the number of data packets that may be served during a time interval [0, t) in the presence of voice traffic, clearly, $C^{D_1'}(t)$ does not have the same distribution as $C^{D_1}(t)$. So according to the definition of energy function in (2.3), we can conclude that $\Lambda_C^{D_1'}(\varphi) \neq \Lambda_C^{D_1}(\varphi)$.

Unfortunately, we have not been able to determine $C^{D_1'}(t)$ thus cannot obtain $\Lambda_C^{D_1'}(\varphi)$. It is another common bottleneck in a multi-priority queuing system to determine the number of departures during a certain period for a low priority traffic, since it is very complicated and most of the time there does not exist a closed form expression. As a result of that, we propose the following approximation. Assuming

$$C^{D_1'}(t) = C^{D_1}\left(t - \sum_{j=0}^{A^V(t)} 1\right) = C^{D_1}(t) - C^{D_1}\left(A^V(t)\right) \qquad (2.10)$$

where $A^V(t)$ is the number of voice packet arrivals during [0, t) and 1 corresponds to the one slot for transmission of a voice packet. Since service of each voice packet takes one slot, the above equation states that after voice arrival packets have all been served, during [0, t), there is only a period of $t - A^V(t)$ that can be used to serve D_1 packets. And that $t - A^V(t)$ period is exclusive for service for D_1 packets, just as in the sole D_1 case.

As we have shown in (2.9), $C^{D_1}(t)$ can be approximated as a Gaussian random variable with mean $\frac{t}{\mu}$, and variance $\frac{\sigma^2 t}{\mu^3}$. So applying central limit theorem for renewal processes again, we can say $C^{D_1}\left(A^V(t)\right)$ is also another Gaussian rv with mean $\frac{A^V(t)}{\mu}$ and variance $\frac{\sigma^2 A^V(t)}{\mu^3}$ since $A^V(t)$ goes to infinity as *t* goes to infinite. And recall the definition of energy function in (2.3), we could have

$$\Lambda_C^{D_1}{}'(\varphi) = \lim_{t\to\infty}\frac{1}{t} log\, E\left(e^{\varphi C^{D_1}{}'(t)}\right) = \lim_{t\to\infty}\frac{1}{t} logE\left(e^{\varphi C^{D_1}(t) - \varphi C^{D_1}\left(A^V(t)\right)}\right)$$

assuming $C^{D_1}(t)$ and $C^{D_1}\left(A^V(t)\right)$ are independent, we have

$$\begin{aligned}\Lambda_C^{D_1}{}'(\varphi) &\approx \lim_{t\to\infty}\frac{1}{t} logE\left(e^{\varphi C^{D_1}(t)}\right) + \lim_{t\to\infty}\frac{1}{t} log\, E\left(e^{-\varphi C^{D_1}\left(A^V(t)\right)}\right) \\ &= \frac{\varphi}{\mu} + \frac{\varphi^2\sigma^2}{2\mu^3} + \lim_{t\to\infty}\frac{1}{t} log\left(\sum_{G=0}^{\infty} e^{\frac{-G\varphi}{\mu} + \frac{G(-\varphi)^2\sigma^2}{2\mu^3}} Prob\left(A^V(t) = G\right)\right)\end{aligned}$$

noticing that in the above expression, the argument in the log () is the probability generating function (pgf) of $A^V(t)$ and since voice arrival process is a Poisson process with rate λ_V, then we have,

$$\Lambda_C^{D_1}{}'(\varphi) = \frac{\varphi}{\mu} + \frac{\varphi^2\sigma^2}{2\mu^3} + \lim_{t\to\infty}\frac{1}{t} log\left(e^{\lambda_V t(z-1)}\middle| z = e^{\frac{-\varphi}{\mu}+\frac{\varphi^2\sigma^2}{2\mu^3}}\right)$$

$$= \frac{\varphi}{\mu} + \frac{\varphi^2\sigma^2}{2\mu^3} + \lambda_V\left(e^{\frac{-\varphi}{\mu}+\frac{\varphi^2\sigma^2}{2\mu^3}} - 1\right) \tag{2.11}$$

At this point, we have obtained the energy function of departure process of D_1 traffic in the presence of voice in (2.11), by using an approximate method to obtain $C^{D_1}{}'(t)$ in (2.10) and applying the asymptotic method to obtain $\Lambda_C^{D_1}{}'(\varphi)$.

And substituting (2.5) and (2.11), the energy functions of arrival and departure process of D_1 traffic in the presence of voice, into (2.4), we obtain the delay-bound violation probability of D_1 traffic in the presence of voice,

$$Prob(D > D_{th}) \approx e^{-\Lambda_A^{D_1}{}'(\varphi^*)D_{th}} \tag{2.12}$$

where φ^* is the unique solution to the following set of equations,

$$\begin{cases} \Lambda_A^{D_1}{}'(\varphi) + \Lambda_C^{D_1}{}'(-\varphi) = 0 \\ \Lambda_A^{D_1}{}'(\varphi) = \Lambda_A^{D_1} = \lambda_{D_1}(e^{\varphi} - 1) \\ \Lambda_C^{D_1}{}'(\varphi) = \frac{\varphi}{\mu} + \frac{\varphi^2\sigma^2}{2\mu^3} + \lambda_V\left(e^{\frac{-\varphi}{\mu}+\frac{\varphi^2\sigma^2}{2\mu^3}} - 1\right) \\ \mu = \frac{1-p^L}{1-p} \\ \sigma^2 = \frac{-p^{2L} + p^{L+1}(-2L-1) + p^L(-2L+1) + 2p}{(1-p)^2} \end{cases} \tag{2.13}$$

The above equations cannot be solved analytically, but it is possible to solve them numerically using Taylor expansion and that will be explained later on in the numerical results section.

At this point, we have obtained the queuing delay violation probability based on the queuing model described in section 2.1. Next, we are going to extend our analysis to a tri-priority queue to demonstrate our analysis is feasible to any number of priority levels.

2.2.3 Extension of delay violation probability to multiple types of traffic (more than two)

We have obtained the queuing delay violation probability for a dual-priority case in (2.12) and (2.13). The analysis presented above can be easily extended to more than two priorities by repeating the procedures in (2.10) and (2.11) to obtain the energy function of the departure process whenever a new level is involved. For example, assuming there is another data flow D_2 involving in the existing dual-priority queue with the lowest priority. In this case, the queue is a tri-priority queue with voice having the highest priority, D_1 traffic having the middle priority and D_2 traffic having the lowest priority. Clearly, the delay for the D_1 traffic remains the same as before since D_2 traffic is transparent to D_1 and voice. Now, if we want to obtain the queuing delay-bound violation probability for the D_2 traffic, we can do the following work,

Applying the same procedure in (2.10) and (2.11), we then have,

$$C^{D_2{}'}(t) = C^{D_2}\left(t - \sum_{j=0}^{A^V(t)} 1 - \sum_{i=0}^{A^{D_1}(t)} k_i\right) = C^{D_2}(t) - C^{D_2}\left(A^V(t)\right) - C^{D_2}\left(\sum_{i=0}^{A^{D_1}(t)} k_i\right) \quad (2.14)$$

from the definition in former analysis, we know $A^V(t)$ is the number of voice packet arrivals during [0, t), thus similarly we denote $A^{D_1}(t)$ as the number of D_1 packet arrivals during [0, t). For those $A^{D_1}(t)$ arrival packets of data flow D_1, assume that the service time of each of them will take k_i slots where *i* from 0 to $A^{D_1}(t)$, the pgf of k_i is $M_C^{D_1}(z)$ and it is determined in (2.7). Also, we denote $C^{D_2}(t)$ as the number of D_2 packets that may be served during [0, t) if there is no other traffic involved, $C^{D_2}{}'(t)$ the number of D_2 packets that may be served during a time interval [0, t) in the presence of voice traffic and D_1 traffic.

Similar as in (2.10), equation (2.14) can be explained as before: if we subtract the time period that is used for serving voice packets and D_1 packets, the remaining period is then exclusive for the service for D_2 packets.

Let $\Lambda_A^{D_2}(\varphi)$ denotes the energy function of the arrival process of D_2 traffic. Without loss of generality, we assume that D_2 packet arrival process is a Poisson process with arrival rate λ_{D_2} packet/slot, so we have $\Lambda_A^{D_2}(\varphi) = \lambda_{D_2}(e^{\varphi} - 1)$ just like (2.5). And we also assume the saturated departure process of D_2 traffic is a renewal process when no other traffic is involved in the system.

Defining $\Lambda_C^{D_2}(\varphi)$ as the energy function of departure process of D_2 traffic in the sole D_2 case, and it can be defined as $\Lambda_C^{D_2}(\varphi) = lim_{t\to\infty}\frac{1}{t} log\, E\left(e^{\varphi C^{D_2}(t)}\right)$. Since we have assumed that the departure process of D_2 traffic is also a renewal process, using

the central limit theorem for renewal processes again we can obtain an asymptotic result of $\Lambda_C^{D_2}(\varphi)$, which is given by $\Lambda_C^{D_2}(\varphi) = \frac{\varphi}{\mu_{D_2}} + \frac{\varphi^2 \sigma_{D_2}^2}{2\mu_{D_2}^3}$ just like in (2.9), while μ_{D_2} is the mean of the service time of a D_2 packet and ${\sigma_{D_2}}^2$ the variance. Define $\Lambda_C^{D_2}{}'(\varphi)$ as the energy function of the departure process of D_2 traffic in the tri-priority case, and it can be expressed as $\Lambda_C^{D_2}{}'(\varphi) = lim_{t\to\infty} \frac{1}{t} log\ E\left(e^{\varphi C^{D_2}{}'(t)}\right)$, Thus, according to (2.14) , we could have,

$$\Lambda_C^{D_2}{}'(\varphi) = \lim_{t\to\infty} \frac{1}{t} log\ E\left(e^{\varphi C^{D_2}{}'(t)}\right)$$

$$= \lim_{t\to\infty} \frac{1}{t} logE\left(e^{\varphi C^{D_2}(t) - \varphi C^{D_2}\left(A^V(t)\right) - \varphi C^{Dat}\left(\sum_{i=0}^{A^{D_1}(t)} k_i\right)}\right)$$

$$\approx \lim_{t\to\infty} \frac{1}{t} log\ E\left(e^{\varphi C^{D_2}(t)}\right) + \lim_{t\to\infty} \frac{1}{t} logE\left(e^{-\varphi C^{D_2}\left(A^V(t)\right)}\right) + \lim_{t\to\infty} \frac{1}{t} logE\left(e^{-\varphi C^{D_2}\left(\sum_{i=0}^{A^{D_1}(t)} k_i\right)}\right)$$

$$= \frac{\varphi}{\mu_{D_2}} + \frac{\varphi^2 {\sigma_{D_2}}^2}{2{\mu_{D_2}}^3} + \lim_{t\to\infty} \frac{1}{t} log\left(\sum_{G=0}^{\infty} e^{\frac{-G\varphi}{\mu_{D_2}} + \frac{G\varphi^2 {\sigma_{D_2}}^2}{2{\mu_{D_2}}^3}} Prob(A^V(t) = G)\right)$$

$$+ \lim_{t\to\infty} \frac{1}{t} log\left[\sum_{H=0}^{\infty} e^{\frac{-H\varphi}{\mu_{D_2}} + \frac{H\varphi^2 {\sigma_{D_2}}^2}{2{\mu_{D_2}}^3}} Prob\left(\sum_{i=0}^{A^{D_1}(t)} k_i = H\right)\right]$$

$$= \frac{\varphi}{\mu_{D_2}} + \frac{\varphi^2 {\sigma_{D_2}}^2}{2{\mu_{D_2}}^3} + \lim_{t\to\infty} \frac{1}{t} log\left(e^{\lambda_V t(y-1)} \middle| y = e^{\frac{-\varphi}{\mu_{D_2}} + \frac{\varphi^2 {\sigma_{D_2}}^2}{2{\mu_{D_2}}^3}}\right)$$

$$+ \lim_{t\to\infty} \frac{1}{t} log\left(e^{\lambda_{D_1} t(z-1)} | z = M_C^{D_1}(e^{\frac{-\varphi}{\mu_{D_2}} + \frac{\varphi^2 {\sigma_{D_2}}^2}{2{\mu_{D_2}}^3}})\right)$$

$$= \frac{\varphi}{\mu_{D_2}} + \frac{\varphi^2 {\sigma_{D_2}}^2}{2{\mu_{D_2}}^3} + \lambda_V \left(e^{\frac{-\varphi}{\mu_{D_2}} + \frac{\varphi^2 {\sigma_{D_2}}^2}{2{\mu_{D_2}}^3}} - 1\right) + \lambda_{D_1}\left(e^{M_C^{D_1}(z)} - 1\right) \Bigg| z = e^{\frac{-\varphi}{\mu_{D_2}} + \frac{\varphi^2 {\sigma_{D_2}}^2}{2{\mu_{D_2}}^3}} \quad (2.15)$$

$e^{\lambda_{D_1} t(z-1)}$ is the pgf of the Poisson packet arrival process of D_1 traffic with rate λ_{D_1}.

At this point, we have obtained the energy function of the departure process of D_2 packet in the presence of voice and D_1 traffic. So we can determine the delay violation probability for the D_2 traffic by substituting $\Lambda_A^{D_2}{}'(\varphi)$ and $\Lambda_C^{D_2}{}'(\varphi)$ into (2.4) in the same way as (2.12) and (2.13).

From above, we can see our analysis is feasible for a tri-priority queuing system with any arrival and departure processes, as long as those processes are renewal processes which allow application of the central limit theorem for renewal processes to obtain the asymptotic energy function of them.

Next, we summarize the procedure for application of the analysis to obtain the delay violation probability of a traffic in a queuing system with any number of priority levels,

1. Determine the energy function of the saturated departure process of the target traffic with no other traffic involved using the central limit theorem for renewal processes.
2. Use the approximation method in (2.10) or (2.14) to obtain the number of departures of the target traffic in the presence of other traffic by subtracting the time that is used for higher level traffics.
3. Obtain the energy function of the departure process of the target traffic with all other traffic involved by substituting the result from step 2.
4. Obtain the energy function of the arrival process of the target traffic using direct

analysis or asymptotic analysis from central limit theorem for renewal processes.

5. Substitute the energy function of the arrival/departure processes of the target traffic into (2.4) to achieve the final queuing delay violation probability.

2.3 Numerical results

In this section, we present some numerical results regarding the analysis of the dual-priority queue we have analyzed before.

First, we present the delay violation probabilities as a function of the delay threshold for the D_1 traffic in Fig.s 2.2, 2.3 and 2.4 with λ_V, λ_{D_1}, p and L as parameters. From the figures, as expected, probability of delay violation increases as λ_{D_1}, λ_V, p or L increases. In Fig.s 2.4a, b the values of the outage probability is p=0.1 and 0.2 respectively and in Fig. 2.4a, the dashed curves corresponds to L = 4 and 8 which overlaps with each other. This is because the retransmissions occur rarely since the probability of outage has a low value, p = 0.1 and, as a result, the value of L does not affect the delay much. However, in Fig. 2.4b it may be seen that the delay violation probability increases sharply with L rising from 2 to 4. This is because of higher value of the outage probability the retransmissions occur more frequently, which results in higher delays.

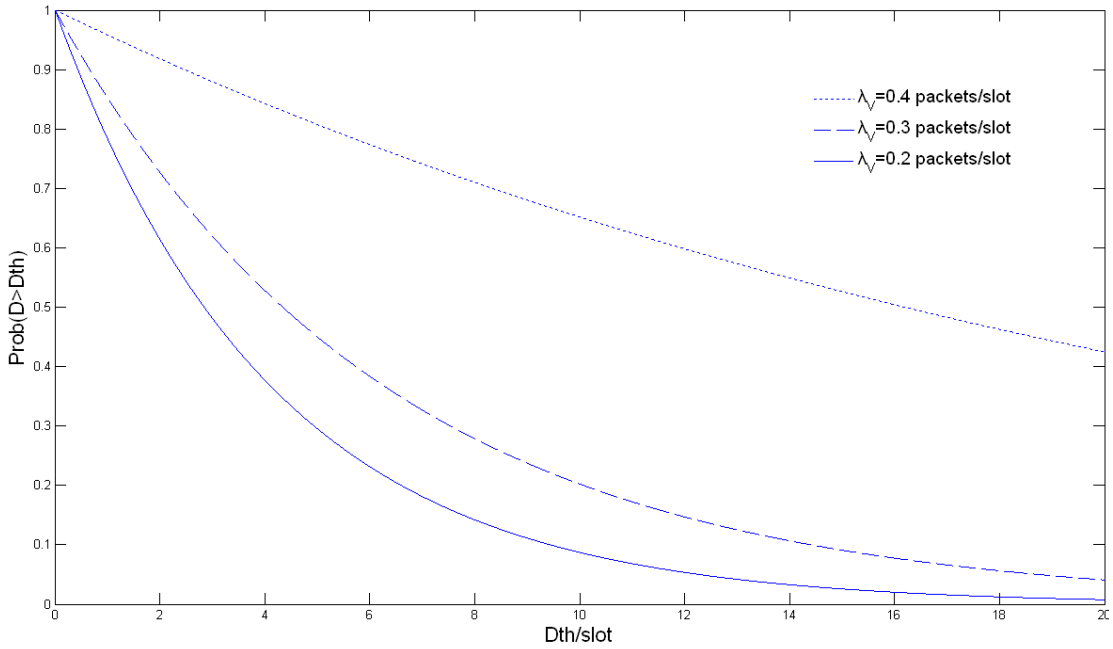

Fig. 2.2. Probability of queuing delay being greater than a threshold value D_{th}, for $\lambda_{D_1} = 0.5$ packets/slot, $p = 0.1, L = 4$ with respect to (wrt) different values of λ_v

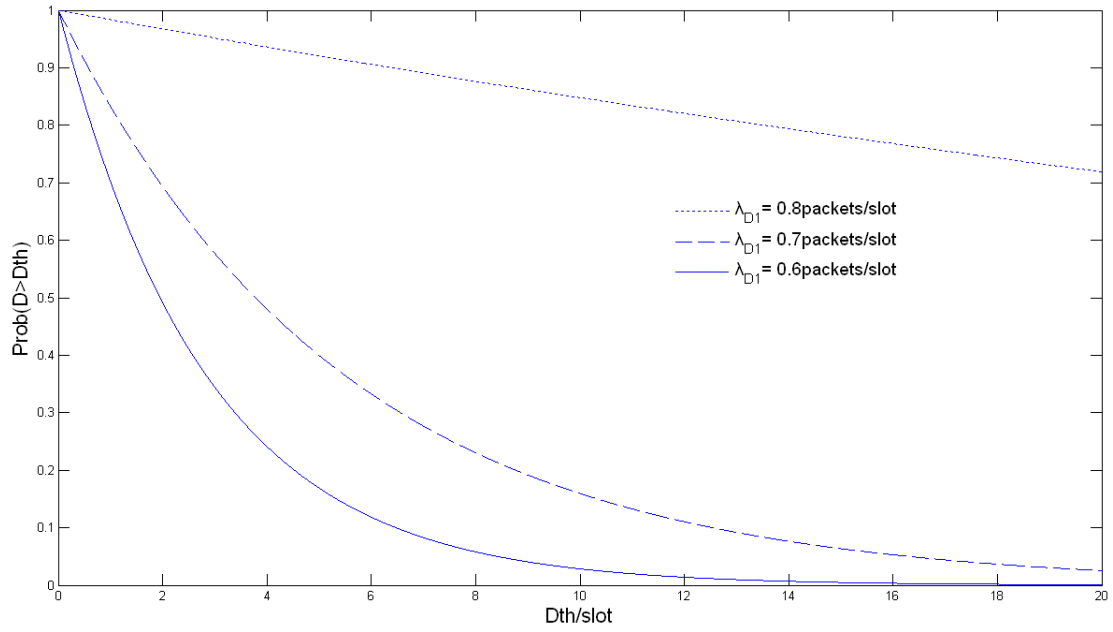

Fig. 2.3. Probability of queuing delay being greater than a threshold value D_{th}, for $\lambda_V = 0.1$ packets/slot, $p = 0.1, L = 4$ wrt to different values of λ_{D_1}

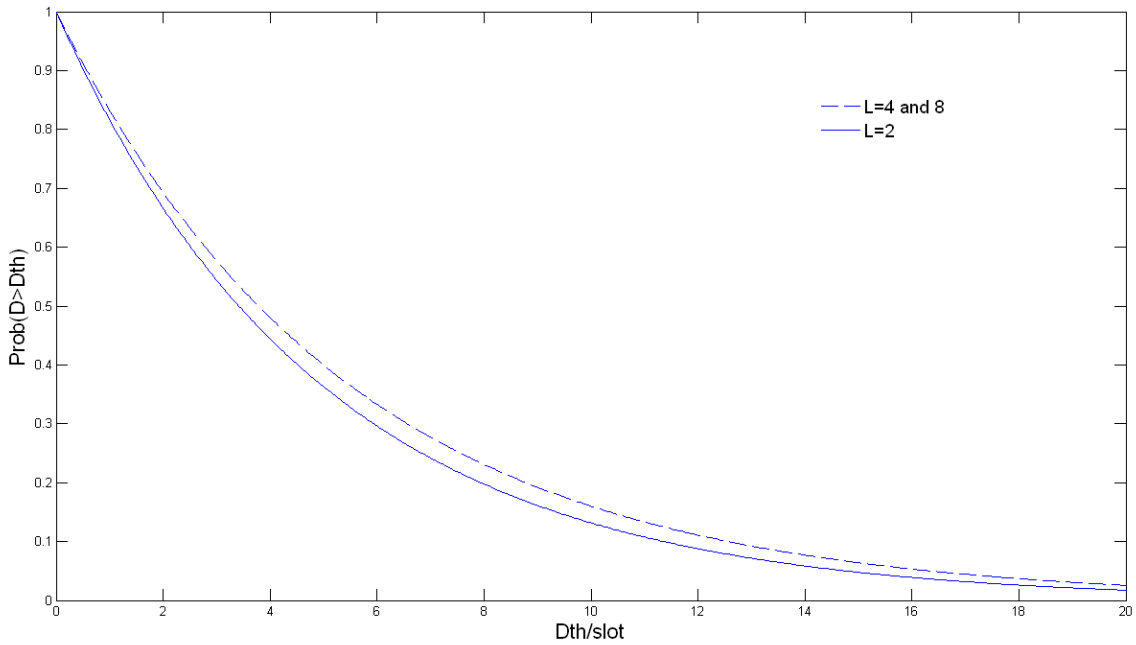

(a) $p = 0.1$

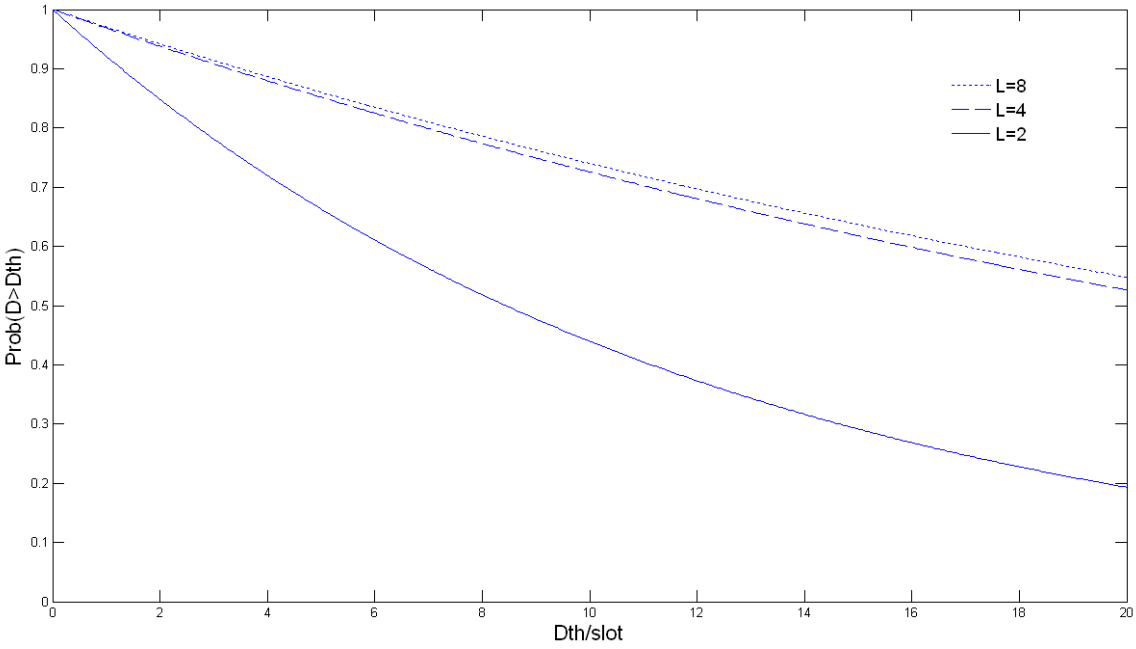

(b) $p = 0.2$

Fig. 2.4. Probability of queuing delay being greater than a threshold value D_{th}, for $\lambda_{D_1} = 0.7$ packets/slot, $\lambda_V = 0.1$ packets/slot, wrt different transmission time L and outage probability p

Fig. 2.5 presents packet loss probability as a function of the allowed maximum number of transmissions of a packet, L, with probability outage p as a parameter. As may be seen, packet loss probability decreases as L increases for fixed values of p. On the

other hand, packet loss probability increases as p increases for fixed values of L. We note that results in this figure will also apply to voice for L=1.

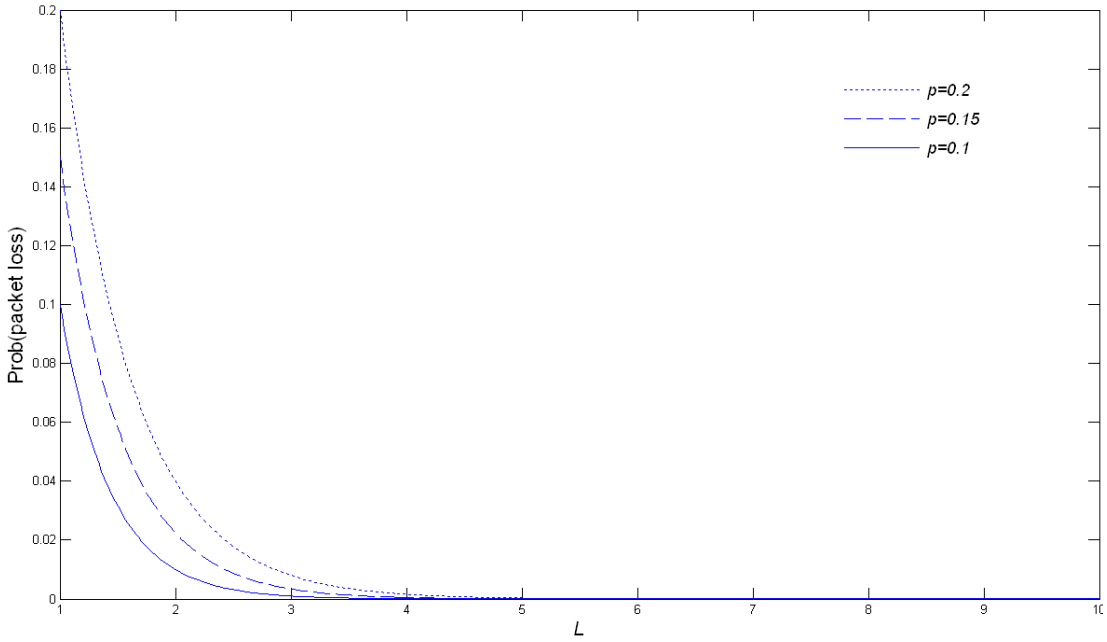

Fig. 2.5. Probability of packet loss as a function of maximum number of transmissions of a packet, L, wrt different outage probability p

Next, we discuss the tradeoffs between queuing delay, packet loss and probability of outage. From Fig.s 2.4 and 2.5, we can reduce the packet loss probability for traffics by increasing the number of transmission attempts, L, but, unfortunately, this also increases the queuing delay. On the other hand, decrease in the probability of outage will result in the reduction of both packet loss as well as the queuing delay. Also, decrease in outage probability can also reduce the retransmission times thus save bandwidth and energy. So a small outage probability is very crucial, in any wireless networks. And that's why we continue the work to obtain the optimum antenna layout that achieves the minimum average outage probability of the DAS in Chapter 3.

2.4 Simulation results

In this section we are going to present two simulation results for analysis of the dual-priority queue in Figs 2.6 and 2.7. From the figures, we can see that simulation and numerical computation matches perfectly well with each other. There are some slightly differences between those two, that reason would be that randomness is hard to be simulated appropriately in computer. Another reason might be using the central limite theorem for renewal process to calculate the asymptotic energy function in (2.9), though we have shown in Fig. 2.1 that for small φ it is a very good approximation, little difference is still there. Also the approximate method used in equation (2.10) in calculating the number of departures of a low priority traffic will introduce some error. And in (2.11), since $C^{D_1}\left(A^V(t)\right)$ and $C^{D_1}(t)$ are not independent form each other so there exists another approximation there, which is represented below,

$$\lim_{t\to\infty}\frac{1}{t}logE\left(e^{\varphi C^{D_1}(t)-\varphi C^{D_1}\left(A^V(t)\right)}\right)=\lim_{t\to\infty}\frac{1}{t}log\left(e^{\varphi C^{D_1}(t)}\right)+\lim_{t\to\infty}\frac{1}{t}log\left(e^{-\varphi C^{D_1}\left(A^V(t)\right)}\right)$$

Despite all those approximations, comparisons of the results show that our analysis still works perfectly for a multi-priority queuing system under heavy traffic load. Further, the developed method can be applied to any generalized multi-priority queue with any renewal arrive/departure processes, even whose energy functions are hard to obtain.

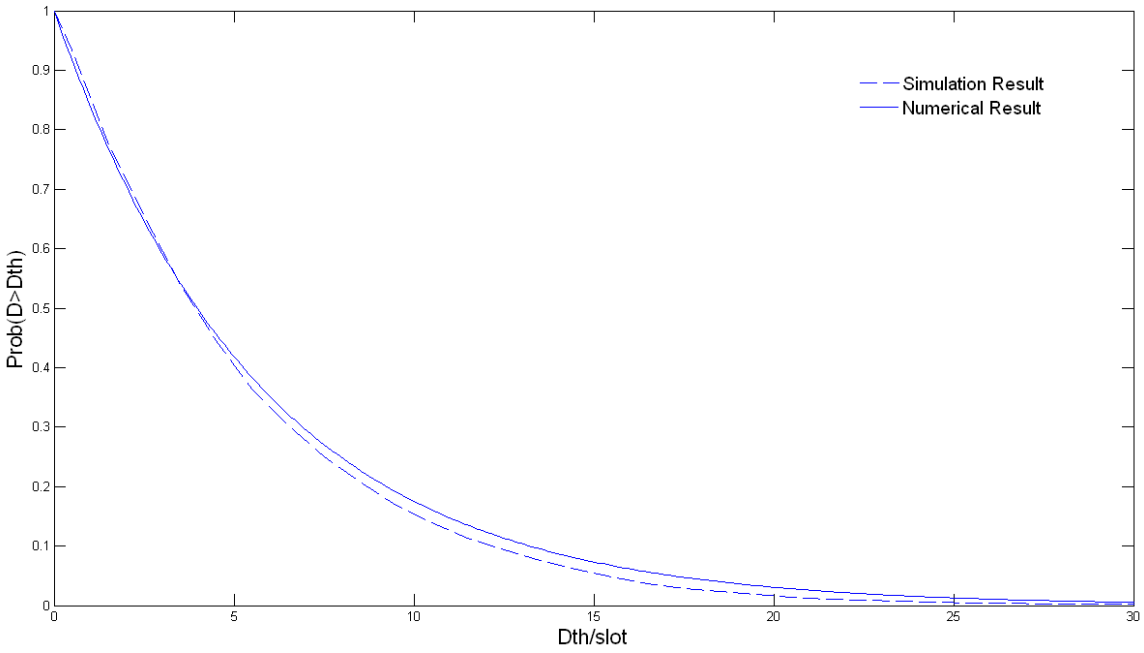

Fig. 2.6. Simulation and numerical results of probability of queuing delay being greater than a threshold value D_{th}, for $\lambda_{D_1} = 0.6$ packets/slot, $\lambda_V = 0.2$ packets/slot, $p = 0.1$, $L = 4$

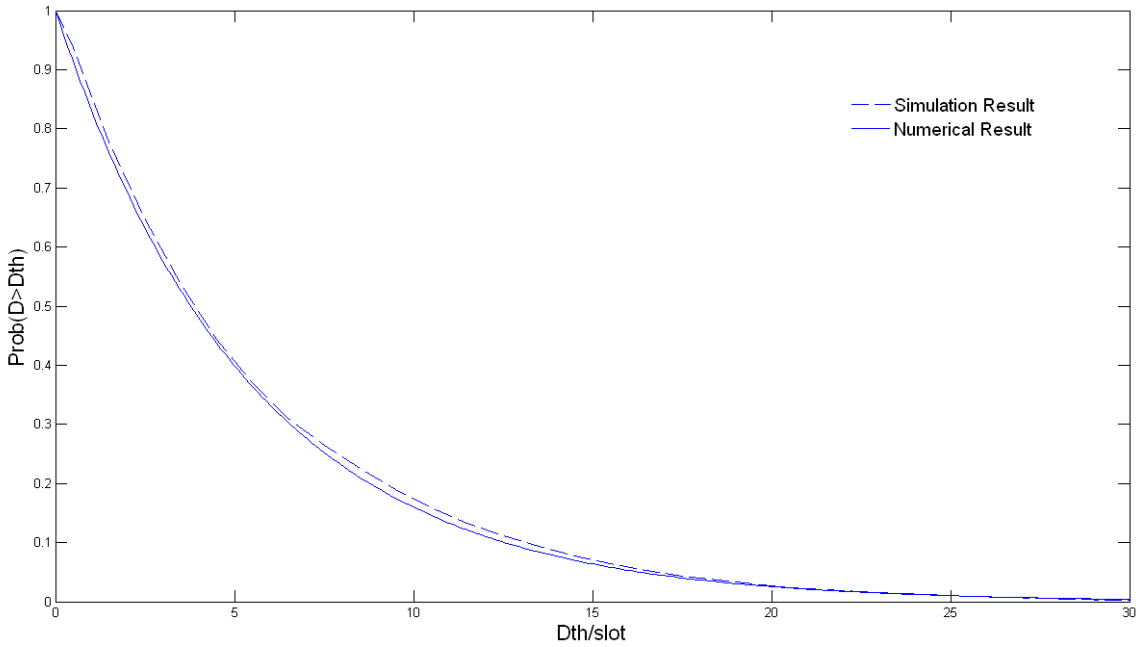

Fig. 2.7. Simulation and numerical results of probability of queuing delay being greater than a threshold value D_{th} for $\lambda_{D_1} = 0.7$ packets/slot, $\lambda_V = 0.1$ packets/slot $p = 0.1$, $L = 4$

Chapter 3. Optimal placement of antennas in DAS

As known from the previous chapter, the outage probability is an important QoS metric, the reduction of it can reduce the queuing delay together with the packet loss probability, and at the same time help increase the bandwidth and the power efficiencies. In this chapter, we aim to obtain the optimal locations of distributed antennas in distributed antenna system (DAS) such that the system's average uplink outage probability is minimized. Due to large mathematic difficulties, closed form expression of optimum antenna layout could not be obtained, instead, numerical and simulation results are given.

3.1 System model

In the section, we will present the system model of distributed broadband wireless communication system (BWC) which contains four subparts: network topology, channel model, frequency reuse mechanism and uplink transmission scheme.

3.1.1 Network topology

First, we will describe the network topology. We will assume the distributed BWC system having a cellular network architecture as shown in Fig. 3.1. In this architecture, cells form clusters. Without loss of any generality, we will assume cluster size *F* to be 7. As shown in Fig. 3.1, the cells in the clustered will be numbered as A_i, *i*=0,…,*F*-1. And we will refer cell A_0 as the target cell.

We show each cell as a circle rather than a hexagon since in reality, cells are mostly in shape of circle, and hexagon is usually used as a theoretical approximation model.

It is assumed that each cell contains a central processor and *M* distributed antennas, which are placed at different geographical locations and each of these antennas is connected to the central processor of its own cell through fiber lines. In Fig. 3.1 only the antennas in the target cell A_0 have been shown to prevent crowding, however, each of the other cells also contains *M* antennas which are deployed in the same manner as in the target cell.

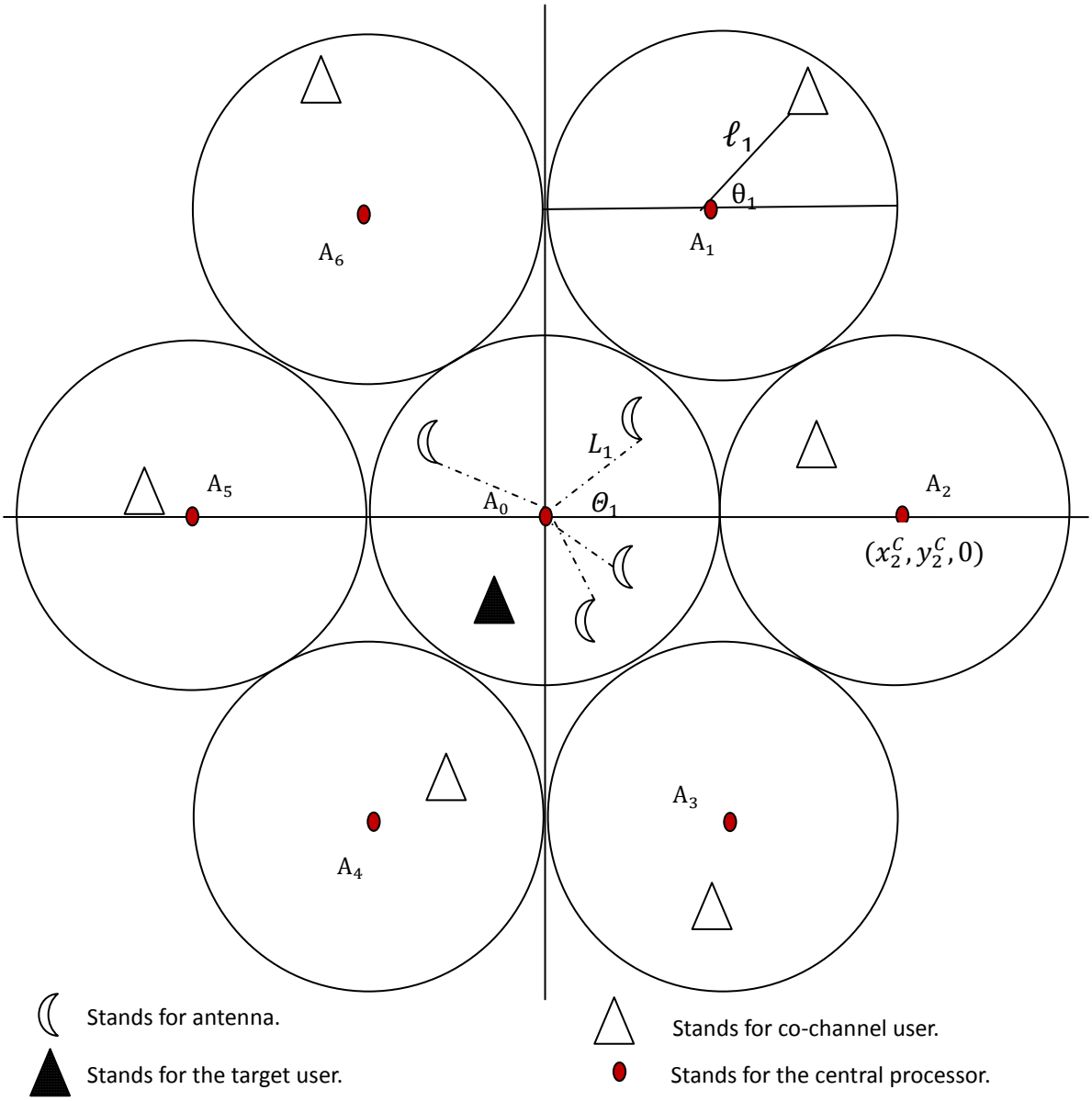

Fig. 3.1: Topology of the distributed BWC system which has a cellular network architecture

All the cells are assumed to have the same size with radius r which has been assigned an unitary value of $r = 1$. The locations of cell A_i's center will be given by $(x_i^C, y_i^C, 0)$, for $i = 0,\ldots, F\text{-}1$, with respect to (wrt) a Cartesian coordinate system located at the center of cell A_0.

In the target cell, locations of the *M* antennas wrt the cell center are denoted by $(L_m, \Theta_m, \hbar)$ in polar coordinate system or $(X_m, Y_m, \hbar)$ in the Cartesian coordinate system, for *m*=1,..., *M* and $0 < \Theta_1 < \Theta_2 < \cdots < \Theta_M < 2\pi$, with the assumption that all the antennas have the same height $\hbar$, and the users are all at the ground level. This assumption ensures that a user will always be in the far-field (will be introduced later in section 3.1.2.1) of any antenna so we are avoiding the near-field antenna gain problem. The relations between $(L_m, \Theta_m, \hbar)$ and $(X_m, Y_m, \hbar)$ can be expressed as,

$$(X_m, Y_m, \hbar) = (L_m \cos(\Theta_m), L_m sin(\Theta_m), \hbar)$$

As will be shown in the frequency reuse mechanism in section 3.1.3, for a specific frequency channel, in each cell A_i, *i*=0…*F*-1, we will assume only a single user can use it and we will refer to that user as user *i*. The location of user *i* in polar coordinates will be given by $(\ell_i, \theta_i, 0)$ relative to the center of its cell. The location of user *i* in Cartesian coordinates will be given by (x_i, y_i) relative to the center of the target cell A_0, which may be expressed as,

$$(x_i, y_i, 0) = \left(x_i^C + \ell_i \cos\theta_i , y_i^C + \ell_i \sin\theta_i , 0\right)$$

Let $\rho_{m,i}$ denote the distance from mobile user *i* to the m^{th} antennas in the target cell, and it can be written as:

$$\rho_{m,i} = \sqrt{(x_i - X_m)^2 + (y_i - Y_m)^2 + \hbar^2} \qquad (3.1)$$

for $i = 0, 1, \ldots, F-1$, m=1,…M.

3.1.2 Channel model

We assume the uplink channel contains two types of fading, one is large-scale fading due to path loss and the other is small-scale fading due to multipath propagation effects. The combined model of these two fadings is then taken as the channel model.

3.1.2.1 Large-scale fading

The large scale fading refers to the drop of the received local average signal power as a function of the distance between transmitter and receiver pair [14]. The large scale fading is determined by the path-loss model below:

$$p_d = p_{d_0} + 10\eta log\left(\frac{d}{d_0}\right) + \chi_\nu$$

p_d and p_{d_0} are the received local average signal powers at receiver with distances d_1 and d_0 away from the transmitter (in dB). In our case, we consider uplink communications from user to antenna so receiver/transmitter pair refers to antenna/user.

Environment	Path Loss Exponent, η
Free Space	2
Urban area cellular radio	2.7 to 3.5
Shadowed urban cellular radio	3 to 5
In building line-of-sight	1.6 to 1.8
Obstructed in building	4 to 6
Obstructed in factories	2 to 3

Table 3.1: Path loss exponents for some typical environments [16]

d_0 is the far field distance and d cannot be smaller than d_0. "The far field distance is related to largest linear dimension of the transmitter antenna aperture and the carrier wavelength" [16]. Far field distance is determined because when the distance between the transmitter and the receiver is less than the far field distance, the received local average signal power does not follow the above model. Usually, the far field distance is less than 1km for a large cell and 100m for microcells [15]

η is the path loss exponent and is usually chosen between 2 to 6, depends on the channel condition[16]. Table 3.1 presents the values of η in some typical environments.

X_ν is a Gaussian rv with variance ν^2(in dB) representing shadowing, which is not considered in this thesis due to its numerical complexity, just like in [11].

3.1.2.2 Small-scale fading

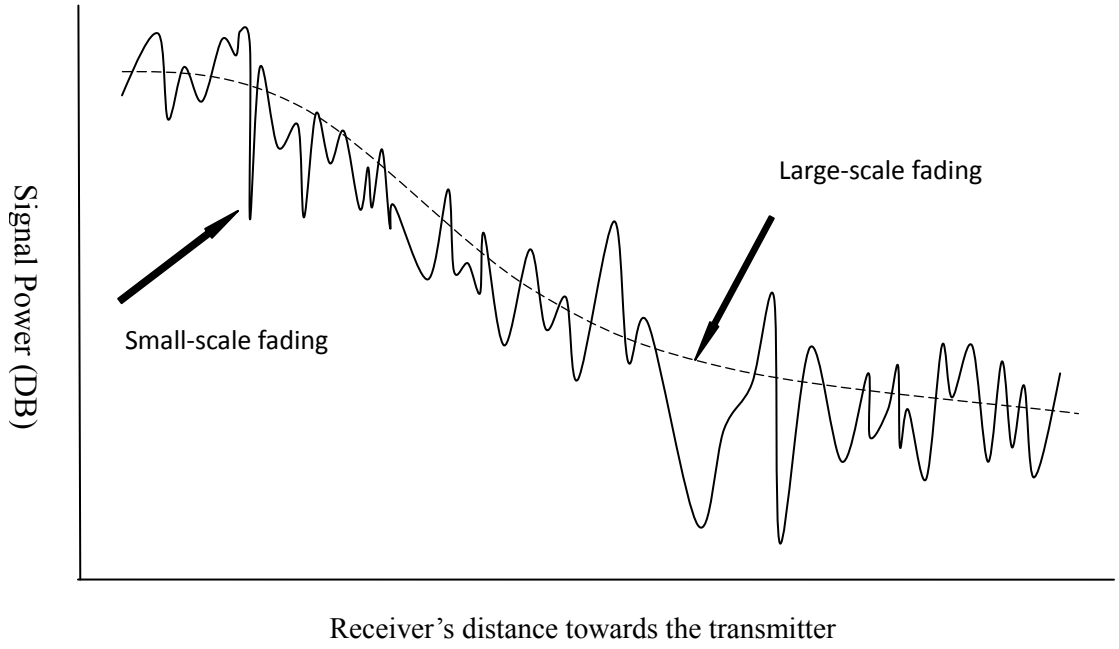

Figure 3.2: Small-scale fading superimposed on large-scale fading [15]

Small scale fading results from the multipath propagation effects in wireless communications which may be caused by the little relative motion between the receiver and transmitter pair, the presence of reflecting and obstructing objects in the channel or the movements of them [14].

When there are large amount of multipath components and no line-of-sight (LoS) component, the received signal power with small-scale fading has a Rayleigh distribution [15]. This kind of small-scale fading model is also called Rayleigh fading model.

A good illustration of a combined large and small scale fading effect is presented

in Figure 3.2 [15]. And we will drive the expression for this channel model below.

Assuming that when a user is transmitting at distance 1 from an antenna, the average received signal strength at the antenna is *W*. Then $S_{m,i}$, the received signal strength at the antenna *m* from any user *i* can be written as,

$$S_{m,i} = W(\rho_{m,i})^{-\eta}\left|h_{m,i}\right|^2 + \varepsilon \tag{3.2}$$

where η is the path loss exponent represents for the large-scale fading. $h_{m,i}$ is an identical independently distributed (i.i.d) normalized complex Gaussian random variable which represents the Rayleigh fading model and ε the noise.

3.1.3 Frequency reuse mechanism

In this section, we will describe the frequency reuse model.

In a cellular network, usually there is a frequency reuse factor of $1/F$ for a conventional cluster with *F* cells, just like the example in section 1.2.1. However, this results in low spectrum efficiency. On the other hand, the increase of reuse factor results in large co-channel interference. In this work, we assume aggressive frequency reuse mechanism, with all the frequencies being available in every cell, or we can say that the reuse factor is 1, as in [10]. The available spectrum will be divided into channels, each

user may be using a single channel at any time. We also assume that the system is saturated so that at any time, all the channels will be busy.

In a cellular system, the major cause of an outage is the co-channel interference from the nearest cells [12]. Let us consider the user in the target cell A_0, which will be referred as the target user. The co-channel interferences to the target user will come from the single user using the same channel in each of the other cells in the cluster. In this work, we treat the inter-cell interferences from the *F*-1 tier one neighboring users as the only source of noise to a target user as well as the only cause of an outage, so ε in (3.2) is assumed to be zero.

So the instantaneous SIR Γ_m at the antenna *m* can be written as,

$$\Gamma_m = \frac{S_{m,0}}{\sum_{i=1}^{F-1} S_{m,i}} \tag{3.3}$$

where $S_{m,i}$ is determined in (3.2) with ε has a zero value.

$S_{m,0}$ is the useful signal power from the target user 0. $\sum_{i=1}^{F-1} S_{m,i}$, the co-channel interferences from other co-channel users, are taken as the only source of noise and are assumed to be the only cause of outage as mentioned before. So Γ_m in fact is also the SNR at the antenna *m*.

3.1.4 Uplink transmission scheme

A user will broadcast its packet which will be received by the antennas in its cell, the received signals will be locally decoded by those antennas and, the results will be forwarded to the central processor through fiber lines, respectively. If at least one of the antennas can decode the packet successfully, the central processor will receive the transmitted packet correctly (local decoding in section 1.2.4). Then, the central processor will take certain action towards processing the result, for example, it may send the result to its affiliated antennas to perform a downlink action or it may pass the result to another central processor to perform a handover.

On the other hand, if none of the antennas is able to decode the packet successfully, then the central processor cannot receive the transmitted packet and this is treated as an outage.

3.2 Outage probability of a single antenna with a given set of user locations

In this section, we are going to present the analysis of $P_m(outage)$, the outage probability of the m^{th} antenna with a given set of user locations $(\boldsymbol{\ell}, \boldsymbol{\theta}, \mathbf{0})$, which is defined as vector $(\boldsymbol{\ell}, \boldsymbol{\theta}, \mathbf{0}) = \{(\ell_0, \theta_0, 0), (\ell_1, \theta_1, 0), \dots, (\ell_{F-1}, \theta_{F-1}, 0)\}$. In section 3.2.1,

we will determine a general expression of $P_m(outage)$. Then, in section 3.2.2 and 3.2.3 we will perform mathematic analysis to get a closed form expression through application of Laplace transforms.

3.2.1 General expression of $P_m(outage)$

First, we are going to derive a general expression of $P_m(outage)$.

For a communication system, outage probability is generally given by [18]:

$$P(outage) = P(I < R) \tag{3.4}$$

where *R* is the required transmission rate of user in bits/sec/Hz [11] and *I* denotes the mutual information of the channel between the transmitter/receiver pair and *I* can be expressed as [19],

$$I = log\ (1 + \Gamma) \tag{3.5}$$

where Γ is the instantaneous SNR at the receiver side.

Substituting (3.5) into (3.4), the outage probability at antenna *m* for a specific user locations set $(\boldsymbol{\ell}, \boldsymbol{\theta}, \mathbf{0})$, can be written as:

$$P_m(outage) = P[log(1 + \Gamma_m) < R] = P(\Gamma_m < 2^R - 1) \tag{3.6}$$

Substituting (3.1), (3.2) and (3.3) into (3.6), we could have:

$$\begin{cases} P_m(outage) = P(\Gamma_m < 2^R - 1) \\ \Gamma_m = \frac{S_{m,0}}{\sum_{i=1}^{F-1} S_{m,i}} \\ S_{m,i} = W\left(\rho_{m,i}\right)^{-\eta} \left|h_{m,i}\right|^2 \\ \rho_{m,i} = \sqrt{(x_i - X_m)^2 + (y_i - Y_m)^2 + \hbar^2} \\ (x_i, y_i, 0) = \left(x_i^C + \ell_i \cos\theta_i \, , y_i^C + \ell_i \sin\theta_i \, , 0\right) \\ (X_m, Y_m, \hbar) = (L_m \cos(\Theta_m), L_m sin(\Theta_m), \hbar) \end{cases} \tag{3.7}$$

for $i = 0, 1, \ldots, F-1$, m=1,…M.

Let us define random variable (rv) $\mathbb{X}_{m,i}$ as $\mathbb{X}_{m,i} = \frac{S_{m,i}}{W}$ and $\mathbb{Y}_m$ as $\mathbb{Y}_m = \sum_{i=1}^{F-1} \mathbb{X}_{m,i}$. We note that $\mathbb{Y}_m$ is always positive. Then we have,

$$\begin{aligned} P_m(outage) = P(\Gamma_m < 2^R - 1) &= P\left(\frac{\mathbb{X}_{m,0}}{\mathbb{Y}_m} < 2^R - 1\right) \\ &= P\left[(2^R - 1)\mathbb{Y}_m - \mathbb{X}_{m,0} > 0\right] \end{aligned} \tag{3.8}$$

Since $h_{m,i}$ is a normalized complex Gaussian rv, then $\left|h_{m,i}\right|$ has a Rayleigh distribution and $\left|h_{m,i}\right|^2$ is an exponentially distributed rv with mean 1, thus $\mathbb{X}_{m,i}$ is also an exponentially distributed rv with mean $\left(\rho_{m,i}\right)^{-\eta}$ and variance $\left(\rho_{m,i}\right)^{-2\eta}$ [20].

Defining K and $\mathbb{Z}_m$ as $K = (2^R - 1)$, $\mathbb{Z}_m = (K\mathbb{Y}_m - \mathbb{X}_{m,0})$ and substituting it into (3.8), we have $P_m(outage) = P[\mathbb{Z}_m > 0]$. Thus (3.7) can be written as,

$$\begin{cases} P_m(outage) = P[\mathbb{Z}_m > 0] \\ \mathbb{Z}_m = \left(K\mathbb{Y}_m - \mathbb{X}_{m,0}\right) \\ \mathbb{Y}_m = \sum_{i=1}^{F-1} \mathbb{X}_{m,i} \\ \mathbb{X}_{m,i} = \left(\rho_{m,i}\right)^{-\eta} * \left|h_{m,i}\right|^2 \\ \rho_{m,i} = \sqrt{(x_i - X_m)^2 + (y_i - Y_m)^2 + \hbar^2} \\ (x_i, y_i, 0) = \left(x_i^C + \ell_i \cos\theta_i\,, y_i^C + \ell_i \sin\theta_i\,, 0\right) \\ (X_m, Y_m, \hbar) = (L_m \cos(\Theta_m), L_m sin(\Theta_m), \hbar) \\ K = (2^R - 1) \end{cases} \tag{3.9}$$

for $i = 0, 1, \ldots, F-1$, m=1,…M.

Equation (3.9) is the general expression of the outage probability of a single antenna m with a given set of user locations $(\boldsymbol{\ell}, \boldsymbol{\theta}, \mathbf{0})$, and it is equal to the probability of rv $\mathbb{Z}_m$ being greater than zero.

3.2.2 The Laplace transform of the rv $\mathbb{Z}_m$

Unfortunately, equation (3.9) does not give us an explicit closed expression for $P_m(outage)$, so in this section and section 3.2.3, we are going to apply Laplace transform techniques to obtain a closed form expression of $P_m(outage)$.

Let $\mathbb{f}_{\mathbb{Z}_m}(x)$ denote the probability density function (pdf) of the random variable $\mathbb{Z}_m$ and $\mathbb{Z}_m(s)$ its Laplace transform.

Define $\mathbb{X}'_{m,0}$ as $\mathbb{X}'_{m,0} = -\mathbb{X}_{m,0}$, $\mathbb{X}'_{m,0}(s)$ its Laplace transform and $\mathbb{f}_{\mathbb{X}'_{m,0}}(x)$ the pdf of $\mathbb{X}'_{m,0}$. From the definition of $\mathbb{Z}_m$ in (3.9), we have,

$$\mathbb{Z}_m = \left(K\mathbb{Y}_m + \mathbb{X}'_{m,0}\right)$$

thus,

$$\mathbb{Z}_m(s) = \mathbb{Y}_m(Ks)\mathbb{X}'_{m,0}(s) \tag{3.10}$$

where $\mathbb{Y}_m(s)$ is the Laplace transform of the rv $\mathbb{Y}_m$.

Since $\mathbb{X}'_{m,0} = -\mathbb{X}_{m,0}$, we have $f_{\mathbb{X}'_{m,0}}(x) = f_{\mathbb{X}_{m,0}}(-x)$, and according to Table 9.1 in [26], we have

$$\mathbb{X}'_{m,0}(s) = \mathbb{X}_{m,0}(-s)$$

where $\mathbb{X}_{m,0}(s)$ is the Laplace transform of the rv $\mathbb{X}_{m,0}$.

So equation (3.10) can be written as,

$$\mathbb{Z}_m(s) = \mathbb{Y}_m(Ks)\mathbb{X}_{m,0}(-s) \tag{3.11}$$

Also rv $\mathbb{Y}_m$ is the sum of $F-1$ independent exponentially distributed rvs $\mathbb{X}_{m,i}$, so we could have,

$$\mathbb{Y}_m(s) = \prod_{i=1}^{F-1} \mathbb{X}_{m,i}(s)$$

where $\mathbb{X}_{m,i}(s) = \frac{(\rho_{m,i})^{\eta}}{s+(\rho_{m,i})^{\eta}}$ since $\mathbb{X}_{m,i}$ is an exponentially distributed rv with mean $(\rho_{m,i})^{-\eta}$ and variance $(\rho_{m,i})^{-2\eta}$.

Then substituting $\mathbb{Y}_m(s)$ and $\mathbb{X}_{m,0}(s)$ into (3.11), we have,

$$\mathbb{Z}_m(s) = \mathbb{Y}_m(KS)\mathbb{X}_{m,0}(-s) = \frac{(\rho_{m,0})^{\eta}}{-s+(\rho_{m,0})^{\eta}} \left(\prod_{i=1}^{F-1} \frac{(\rho_{m,i})^{\eta}}{Ks+(\rho_{m,i})^{\eta}}\right)$$

$$= \left[-(K)^{-F+1} \prod_{i=0}^{F-1} (\rho_{m,i})^{\eta}\right] \left[\frac{1}{s+\left(-(\rho_{m,0})^{\eta}\right)} \left(\prod_{i=1}^{F-1} \frac{1}{s+\frac{(\rho_{m,i})^{\eta}}{K}}\right)\right] \quad (3.12)$$

The region of converge (ROC) of $\mathbb{Z}_m(s)$ is

$$\left\{max\left[\frac{-(\rho_{m,i})^{\eta}}{K}, i = 1, \dots, F-1\right] < \mathcal{R}e(s) < (\rho_{m,0})^{\eta}\right\}$$

where $\mathcal{R}e(\mathrm{s})$ represent the real part of *s*.

Let us define H_m and $\mathcal{F}_{\mathrm{m}}(\mathrm{s})$ as,

$$H_m = -\prod_{i=0}^{F-1} (\rho_{m,i})^{\eta} (K)^{-F+1} \quad (3.13)$$

$$\mathcal{F}_m(s) = \frac{1}{s+\left(-(\rho_{m,0})^{\eta}\right)} \left(\prod_{i=1}^{F-1} \frac{1}{s+\frac{(\rho_{m,i})^{\eta}}{K}}\right) = \prod_{n=1}^{N} \frac{1}{(s+c_{m,n})^{q_n}} \quad (3.14)$$

where $c_{m,n}$, q_n denote a distinct value and its frequency in the set $\{-(\rho_{m,0})^{\eta}, \frac{1}{K}(\rho_{m,1})^{\eta} \dots, \frac{1}{K}(\rho_{m,F-1})^{\eta}\}$ where $n = 1, \dots, N$ with $1 \le N \le F$. We also assume $-(\rho_{m,0})^{\eta} = c_{m,1}$ since $c_{m,1}$ is the only value less than zero and we have $q_1 = 1$.

Substituting (3.13) and (3.14) into (3.12), then we have

$$\mathbb{Z}_m(s) = H_m \mathcal{F}_m(s) \tag{3.15}$$

At this point, we have obtained the Laplace transform of $\mathbb{Z}_m(s)$.

3.2.3 The inverse transform of $\mathbb{Z}_m(s)$ and $P_m(outage)$

Next, we are going to invert $\mathbb{Z}_m(s)$ to obtain $f_{\mathbb{Z}_m}(x)$ and the closed form expression of $P_m(outage)$.

Using partial fraction expansion in $\mathcal{F}_m(s)$ that we had in (3.14), we could have

$$\mathcal{F}_m(s) = \sum_{n=1}^{N} \sum_{j=1}^{q_n} \frac{b_{m,n}^{j}}{(s+c_{m,n})^{j}} \tag{3.16}$$

where $b_{m,n}^{j} = \frac{1}{(j-1)!} \frac{d^{j-1}[(s+c_{m,n})^{j}\mathcal{F}_m(s)]}{ds^{j-1}}\Big| (s = -c_{m,n})$, pleases notice that j in $b_{m,n}^{j}$ is the superscript, not for power.

Then taking the inverse transform of $\mathcal{F}_m(s)$ in (3.16) and then of (3.15), we obtain $f_{\mathbb{Z}_m}(x)$, the pdf of the rv $\mathbb{Z}_m$,

$$f_{\mathbb{Z}_m}(x) = H_m \left\{ q_1 b_{m,1}^{1} e^{-c_{m,1}x} u[-x] + \sum_{n=2}^{N} \sum_{j=1}^{q_n} \frac{b_{m,n}^{j}}{(j-1)!} x^{j-1} e^{-c_{m,n}x}\, u[x] \right\} \tag{3.17}$$

where $u[x] = \begin{cases} 1 & , \ x \geq 0 \\ 0 & , \ x < 0 \end{cases}$

the reason that there exists a unique term $q_1 b_{m,1}^{1} e^{-c_{m,1}x} u[-x]$ in (3.17) is because that

in (3.14) and (3.16), $c_{m,1}$ is the only one less than zero, so according to the inverse Laplace transform Table 9.2 in [26], we obtain this unique term with a $u[-x]$ while other terms end up with $u[x]$.

Recall that $P_m(outage)$ equals to the integration of $f_{\mathbb{Z}_m}(x)$ from zero to infinite as described in (3.9), by take the integration of (3.17), we then have,

$$\begin{aligned} P_m(outage) = P[\mathbb{Z}_m > 0] &= \int_0^{+\infty} f_{\mathbb{Z}_m}(x)dx \\ &= H_m \int_0^{+\infty} \left[b_{m,1}^1 e^{-c_{m,1}x} u[-x] + \sum_{n=2}^{N} \sum_{j=1}^{q_n} \frac{b_{m,n}^j}{(j-1)!} x^{j-1} e^{-c_{m,n}x} u[x] \right] dx \\ &= H_m \sum_{n=2}^{N} \sum_{j=1}^{q_n} \frac{b_{m,n}^j}{\left(c_{m,n}\right)^j} \end{aligned} \tag{3.18}$$

where coefficients $b_{m,n}^j$ were presented in equation (3.16).

By now, we have obtained the closed form expression of $P_m(outage)$ in (3.18).

3.3 Expected outage probability for the system

In this section, we extend the single antenna outage probability $P_m(outage)$ derived in the previous section to the entire system. We determine $\mathbb{P}(outage)$, the system outage probability with a specific user locations set $(\boldsymbol{\ell}, \boldsymbol{\theta}, \mathbf{0})$, and average or expected system outage probability $E(\mathbb{P})$, by averaging $\mathbb{P}(outage)$ with respect to user locations.

Since outage of the antennas are assumed to be independent of each other, the total outage probability of a cell with *M* antennas with a specific set of $(\boldsymbol{\ell}, \boldsymbol{\theta}, \mathbf{0})$ is given by,

$$\mathbb{P}(outage) = \prod_{m=1}^{M} P_m(outage) \tag{3.19}$$

Next, unconditioning the above result wrt the user locations vector $(\boldsymbol{\ell}, \boldsymbol{\theta}, \mathbf{0})$, we can obtain the average or expected outage probability for the system ergodically,

$$\begin{aligned} E(\mathbb{P}) = E_u\big(\mathbb{P}(outage)\big) &= \int_{(\boldsymbol{\ell},\boldsymbol{\theta},\mathbf{0})} \mathbb{P}(outage) p(\boldsymbol{\ell}, \boldsymbol{\theta}, \mathbf{0}) d(\boldsymbol{\ell}, \boldsymbol{\theta}, \mathbf{0}) \\ &= \underbrace{\iiint}_{\ell_i=0\ldots}^{1} \ldots \underbrace{\iiint}_{\theta_i=0\ldots}^{2\pi} \mathbb{P}(outage) \prod_{i=0}^{F-1} p(\ell_i)\, p(\theta_i) d\,\ell_i d\theta_i \end{aligned} \tag{3.20}$$

where $p(\ell_i), p(\theta_i)$ are the marginal pdfs of the coordinates of user *i*, ℓ_i and θ_i respectively, $E_u()$ denotes the expected value wrt the locations of the users. And since we are assuming that users are uniformly distributed in a cell, we have the cumulative distribution function (cdf) for rv ℓ_i as $Prob(\ell_i < \ell) = \frac{\ell^2}{r^2}$, and substituting *r*=1 into it, we have,

$$\begin{cases} p(\ell_i) = 2\ell_i, for\ 0 \le \ell_i \le 1 \\ p(\theta_i) = \frac{1}{2\pi}, for\ 0 \le \theta_i < 2\pi \end{cases} \tag{3.21}$$

Substituting (3.21) into (3.20), we have

$$E(\mathbb{P}) = \left(\frac{1}{\pi}\right)^F \underbrace{\iiint}_{\ell_i=0\ldots}^{1} \ldots \underbrace{\iiint}_{\theta_i=0\ldots}^{2\pi} \mathbb{P}(outage) \prod_{i=0}^{F-1} \ell_i \,(d\ell_i d\theta_i)$$

Thus in all we have,

$$\begin{cases} E(\mathbb{P}) = \left(\frac{1}{\pi}\right)^F \iiint_{\ell_i=0\ldots}^{1} \ldots \iiint_{\theta_i=0\ldots}^{2\pi} \mathbb{P}(outage) \prod_{i=0}^{F-1} \ell_i \, (d\ell_i d\theta_i) \\ \mathbb{P}(outage) = \prod_{m=1}^{M} P_m(outage) \\ P_m(outage) = H_m \sum_{n=2}^{N} \sum_{j=1}^{q_n} \frac{b_{m,n}^{j}}{(c_{m,n})^j} \\ H_m = -(K)^{-F+1} \prod_{i=0}^{F-1} (\rho_{m,i})^{\eta} \\ \rho_{m,i} = \sqrt{(x_i - X_m)^2 + (y_i - Y_m)^2 + \hbar^2} \\ b_{m,n}^{j} = \frac{1}{(j-1)!} \frac{d^{j-1}\left[(s+c_{m,n})^j \mathcal{F}_m(s)\right]}{ds^{j-1}} \Big| (s = -c_{m,n}) \\ \mathcal{F}_m(s) = \frac{1}{s-(\rho_{m,0})^{\eta}} \left(\prod_{i=1}^{F-1} \frac{1}{s+\frac{(\rho_{m,i})^{\eta}}{K}} \right) \\ (x_i, y_i, 0) = \left(x_i^C + \ell_i \cos\theta_i \, , y_i^C + \ell_i \sin\theta_i \, , 0\right) \\ (X_m, Y_m, \hbar) = (L_m \cos(\Theta_m), L_m sin(\Theta_m), \hbar) \\ K = (2^R - 1) \end{cases} \tag{3.22}$$

for $i = 0, 1, \ldots, F-1$, m=1,…M.

At this point, we have obtained the average outage probability for the DAS in (3.22) as a function of antenna locations vector $\boldsymbol{L}$, where $\boldsymbol{L}$ is defined as

$$\boldsymbol{L} = [(L_1, \Theta_1, \hbar), \ldots, (L_M, \Theta_M, \hbar)]$$

3.4 The optimal location of antennas

Now that we have the expression of the expected outage probability for the system in (3.22), we will determine the $\boldsymbol{L}'$, the optimal locations vector of these M antennas where

$\boldsymbol{L}' = [(L_1', \Theta_1', \hbar), \ldots, (L_M', \Theta_M', \hbar)]$. The antenna locations vector that minimize the expected outage probability of the system will be defined as optimal.

We can determine the minimum of $E(\mathbb{P})$ by setting the gradient of $E(\mathbb{P})$ in (3.22) to a zero vector: $grad[E(\mathbb{P})] = \mathbf{0}$, wrt to the antennas location vector $\boldsymbol{L}$

$$\frac{\partial E(\mathbb{P})}{\partial \boldsymbol{L}} = \mathbf{0} \tag{3.23}$$

Among all the vectors that satisfy the above equation set, we choose one with the minimum value of $E(\mathbb{P})$ to be the optimum locations of those *M* antennas, $\boldsymbol{L}'$.

We can also use Leibniz differentiation rule to change the order of derivatives and integrations of equation (3.23), and obtain (3.24)

$$\frac{\partial E(\mathbb{P})}{\partial \boldsymbol{L}} = \frac{\partial E_u(\mathbb{P}(outage))}{\partial \boldsymbol{L}} = E_u(\frac{\partial \mathbb{P}(outage)}{\partial \boldsymbol{L}}) = \mathbf{0} \tag{3.24}$$

Again among all the vectors that satisfy the above equation set, we choose one with the minimum value of $E(\mathbb{P})$ to be $\boldsymbol{L}'$.

Unfortunately, due to mathematic complexity, we cannot get a closed form for the optimal locations of antennas with either approach.

Next, we consider the following simplification. Since all the cells are identical in every aspect, we expect the locations of antennas to be symmetric in each cell. This

means that the antennas in a cell will be at the same distance from the cell center and the space between two neighboring antennas will be the same. Thus, it is expected that the antennas will be on a circle centered at the cell center, just as in [6]. This antenna layout is shown in Fig. 3.2, with four antennas in the target cell in a symmetric placement.

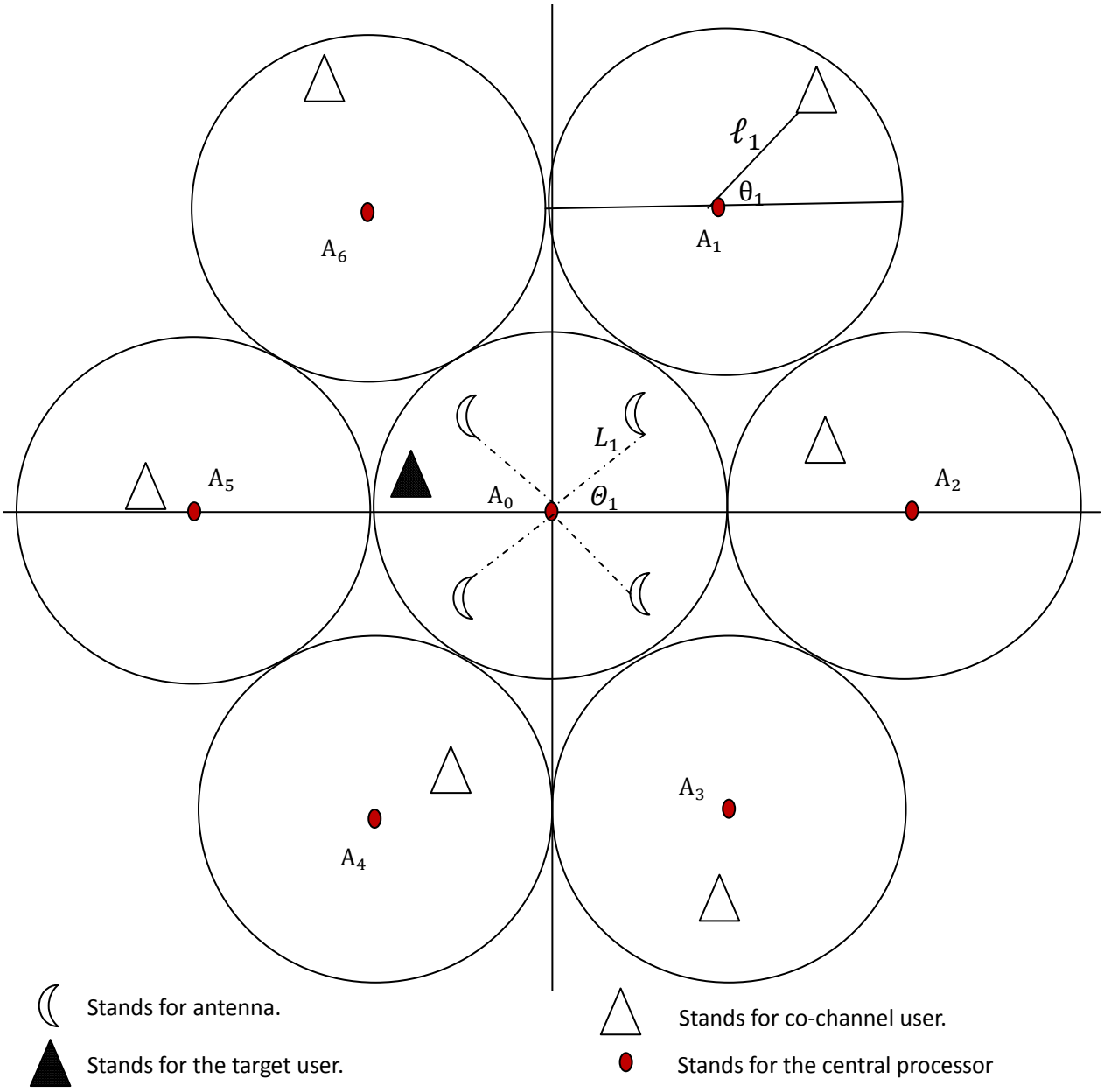

Fig. 3.3: Topology of distributed BWC system with antennas symmetrically deployed on a circle

However, even with this assumption, we could not obtain a closed form due to large mathematic difficulties in performing integrations and derivatives. As a result, we have no choice but to obtain results through numerical calculations and simulations.

3.5 Numerical results

Theoretically, by turning the infinite integrations with respect to the users' locations $(\boldsymbol{\ell}, \boldsymbol{\theta}, \mathbf{0})$ in equation (3.22) into finite numerical accumulations, with the assumption of a circular symmetric antenna layout, we may obtain $E(\mathbb{P})$ with a certain antenna locations vector $\boldsymbol{L}$. And after we apply the above procedure for every possible antenna locations, the vector which achieves the minimum value of $E(\mathbb{P})$ is then our optimum antenna layout, $\boldsymbol{L}'$. Explicitly, the density of possible locations of users and candidate antenna will decide the accuracy of the numerical result.

However, the computation complexity limits us from obtaining accurate numerical results which may require months of computer computations. So below we are going to present a Robbins-Monro iterative algorithm from stochastic approximation theory to obtain the optimum antenna layout.

Before we present the Robbins-Monro procedure, we will first give the system parameters for numerical computations. We assume a circular symmetric antenna layout

with four antennas in a cell, *M*=4, see Fig. 3.3. Antenna's height $\hbar$ is assumed to have value of 0.05, *R* is assumed a value of 1 bits/sec/Hz, η is assumed a value of 4, which is a typical path loss exponent in wireless communication model as in [6]. We will carry the above assumptions and parameters to perform the Robbins-Monro iterative algorithm. Also we define the first antenna with the coordinate $(L_1, \Theta_1, \hbar)$

3.5.1 Brief introduction of Robbins-Monro algorithm

In this section, we are going to give a brief introduction of Robbins-Monro algorithm from stochastic approximation theory.

Robbins-Monro algorithm is an iterative stochastic approximation algorithm. It applies an iterative estimation procedure via noisy observations to find the values or extremes of functions which cannot be obtained directly through regular mathematical analysis [29].

For example, if we have a function $M(x)$ that cannot be observed directly or having a very complicated expression, and we want to obtain the root x' of the equation $M(x) = y$, where *y* is a constant value, we can apply the following procedure iteratively to obtain x',

$$x(n+1) - x(n) = a_n[y - N(x(n))]$$

where $a_1, a_2, \dots, a_n$ is a sequence of positive step sizes and the expected value of function $N(x)$ equals to $M(x)$, which can be expressed as $E\big(N(x)\big) = M(x)$. Or we can say that $N(x)$ is a noisy observation or an unbiased estimator of $M(x)$[10]. And Robbins and Monro proved that $x(n)$ converges to x' as *n* increases, provided that [29],

1. $N(x)$ is uniformly bounded
2. $M(x)$ is non decreasing
3. $M'(x')$ exists and is positive
4. a_n satisfies the following requirements: $\sum_0^\infty a_n = \infty$ *and* $\sum_0^\infty a_n^2 < \infty$

Polyak and Juditsky proposed an improved version of Robbins-Monro algorithm to accelerate the outcome of the above algorithm [30],

$$x(n+1) - x(n) = b_n\big[y - N\big(x(n)\big)\big], \qquad \overline{x(n)} = \frac{1}{n}\sum_{i=0}^{n-1} x(i)$$

and $\overline{x(n)}$ converges to x' given that the constraints 1 to 3 in the above are satisfied and sequence b_n satisfy $b_n \to \infty$ and $\frac{b_n - b_{n+1}}{b_n} = o(b_n)$.

$f(n) = o(g(n))$ represents that $f(n)$ grows much slower than $g(n)$ does, formally, it means that for any positive constant ε there exists a constant N such that [31]

$$|f(n)| \leq \varepsilon|(g(n))|, \text{ for all } n \geq N$$

An example of a such sequence of step size may be $b_n = An^{-a}$, where $0<a<1$, and A is a positive value [30].

3.5.2 Application of Robbins-Monro algorithm in obtaining optimum antenna layout

Using the same procedure described in section 3.5.1, we treat $\frac{\partial \mathbb{P}(outage)}{\partial \boldsymbol{L}}$ as $N(\boldsymbol{L})$ and $\frac{\partial \mathrm{E}(\mathbb{P})}{\partial \boldsymbol{L}}$ as $M(\boldsymbol{L})$ [10]. And from (3.24), which is presented again below, we can tell $N(\boldsymbol{L})$ is an unbiased estimator of $M(\boldsymbol{L})$ and we have $M(\boldsymbol{L}) = E_u(N(\boldsymbol{L}))$.

$$\frac{\partial E(\mathbb{P})}{\partial \boldsymbol{L}} = \frac{\partial E_u\big(\mathbb{P}(outage)\big)}{\partial \boldsymbol{L}} = E_u\left(\frac{\partial \mathbb{P}(outage)}{\partial \boldsymbol{L}}\right) = \mathbf{0}$$

Next, we are going to perform the following Robbins-Monro procedure to obtain the optimum antenna layout similar as in [10],

a. Initial an antennas location vector $\boldsymbol{L}(n)$ and set n=1
b. Randomly generate a users location vector $(\boldsymbol{\ell}, \boldsymbol{\theta}, \mathbf{0})$ according to their uniform distributions in a cell.
c. Upgrade the optimum locations by applying the equation below

$$\boldsymbol{L}(n+1) = \boldsymbol{L}(n) + c_n \left(\frac{\partial \mathbb{P}(outage)}{\partial \boldsymbol{L}} \right) \Bigg| \boldsymbol{L} = \boldsymbol{L}(n)$$

d. Let $n=n+1$ and iteratively run steps *b, c, d* until $\overline{\boldsymbol{L}(n)}$ converges, where $\overline{\boldsymbol{L}(n)} =$

$\frac{1}{n-1}\sum_{i=1}^{n-1}\boldsymbol{L}(i)$. And $\overline{\boldsymbol{L}(n)}$ converges to the optimum antenna location vector $\boldsymbol{L}'$.

In our implementation of Robbins-Monro algorithm, we choose the sequence of positive c_n as $c_n = 15n^{-0.75}$, which satisfies the Polyak and Juditsky constraints described at the end of section 3.5.1.

The outcome is shown below in Table 3.2. Since the antennas are symmetrically located on the circle centered at the cell center, we only consider the first antenna's location with the coordinate $\left(\overline{L_1(n)}, \overline{\Theta_1(n)}, \hbar\right)$, with $\hbar = 0.05$.The locations of the other three antennas can be easily obtained. Since from results, the values of $\overline{\Theta_1(n)}$ are all very close to zero, we are not showing them in the table. So in the following table we only show the results of $\overline{L_1(n)}$, which is also the radius of the antennas circle.

From the table below, we can tell that the $\overline{L_1(n)}$ converges to 0.58. So the optimum location of the first antenna is $(0.58, 0, 0.05)$, and the other three antennas are at locations $(0.58, \frac{\pi}{2}, 0.05)$, $(0.58, \pi, 0.05)$, $(0.58, \frac{3\pi}{2}, 0.05)$ respectively. This optimum antenna layout achieves the minimum average uplink outage probability of the distributed antenna system with the value of 0.0087.

n	$\overline{L_1}$
1	0.00
2	0.90
3	0.63
4	0.54
5	0.50
6	0.47
7	0.45
8	0.46
9	0.48
10	0.49
11	0.50
12	0.50
13	0.50
14	0.51
15	0.51
16	0.51
17	0.51
18	0.51
19	0.52
20	0.52
21	0.52
22	0.52
23	0.53
24	0.53
25	0.53
26	0.54
27	0.54
28	0.54
29	0.54
30	0.54

n	$\overline{L_1}$
31	0.54
32	0.54
33	0.54
34	0.54
35	0.55
36	0.55
37	0.55
38	0.55
39	0.55
40	0.55
41	0.55
42	0.56
43	0.56
44	0.56
45	0.56
46	0.56
47	0.56
48	0.56
49	0.57
50	0.57
51	0.57
52	0.57
53	0.57
54	0.57
55	0.57
56	0.57
57	0.58
58	0.58
59	0.58
60	0.58

n	$\overline{L_1}$
61	0.58
62	0.58
63	0.58
64	0.58
65	0.58
66	0.58
67	0.58
68	0.58
69	0.59
70	0.59
71	0.59
72	0.59
73	0.59
74	0.59
75	0.59
76	0.58
77	0.58
78	0.58
79	0.58
80	0.58
81	0.58
82	0.58
83	0.58
84	0.58
85	0.58
86	0.58
87	0.58
88	0.58

Table 3.2 Robbins-Monro outcome of the optimum location of the first antenna with four antennas in a cell

3.6 Simulation results

We are going to show our simulation results in this section. In section 3.6.1, we will describe our simulation procedures. And the simulation result for a circular symmetric antenna layout is shown in section 3.6.2 with M=4, and from it we can see that numerical and simulation results are close. We will also take a look at the worst case in section 3.6.3. The worst case represents the situation that the co-channel interferences are the most severe, which means that the neighboring users are at the closet locations towards the target cell.

Section 3.6.2 and 3.6.3 are both based on a 4 antennas assumption. We will show the same kind of results for 1,5 antennas in section 3.6.4. And a summary will be given after that in section 3.6.5.

3.6.1 Simulation procedures

The procedure of the Matlab simulation is briefly introduced below.

We apply Monte-Carlo algorithm in the simulation following equation (3.7) and (3.19) which will be rewritten below,

$$\begin{cases} P_m(outage) = P(\Gamma_m < 2^R - 1) \\ \Gamma_m = \frac{S_{m,0}}{\sum_{i=1}^{F-1} S_{m,i}} \\ S_{m,i} = W\left(\rho_{m,i}\right)^{-\eta} \left|h_{m,i}\right|^2 \\ \rho_{m,i} = \sqrt{(x_i - X_m)^2 + (y_i - Y_m)^2 + \hbar^2} \\ (x_i, y_i, 0) = \left(x_i^C + \ell_i \cos\theta_i \, , y_i^C + \ell_i \sin\theta_i \, , 0\right) \\ (X_m, Y_m, \hbar) = (L_m \cos(\Theta_m), L_m sin(\Theta_m), \hbar) \end{cases} \tag{3.7}$$

$$\mathbb{P}(outage) = \prod_{m=1}^{M} P_m(outage) \tag{3.19}$$

We assume the first antenna has the following possibilities locations, L_1 is chosen from (0, 0.05, 0.1,… ,1) and Θ_1 is chosen from (0, $\frac{\pi}{18}$, $\frac{2\pi}{18}$,… ,$\frac{\pi}{2} - \frac{\pi}{18}$). The remaining *M-1* antennas are placed on the circle collocated at the cell center with the radius that equals to the distance of the first antenna and the arc length between the neighboring antennas are equal with the value of $\frac{2\pi}{M}$. Once the location of the first antenna is chosen, the whole topology of DAS is fixed. So there are $21 * 9 = 188$ candidate antenna locations vectors $\boldsymbol{L}$.

For each $\boldsymbol{L}$, I will randomly generating 10000 user locations vector $(\boldsymbol{\ell}, \boldsymbol{\theta}, \mathbf{0})$, according to users' distribution. And for each of these user locations vector, I will calculate the distance $\rho_{m,i}$ and generate exponential rvs vector $\boldsymbol{h_m}$ 1000 times, where $\boldsymbol{h_m} = (h_{m,0}, h_{m,1}, \dots, h_{m,F-1})$ using Matlab times. Then using (3.7), for each $\boldsymbol{h_m}$, I can count the number of events that satisfies

$$(\Gamma_m = \frac{S_{m,0}}{\sum_{i=1}^{F-1} S_{m,i}} < 2^R - 1), \qquad \text{where } S_{m,i} = W\left(\rho_{m,i}\right)^{-\eta} \left|h_{m,i}\right|^2$$

event $\Gamma_m < 2^R - 1$ means an outage occurs at antenna m. Dividing the number of outage events by 1000, then that's our $P_m(outage)$ with one specific user locations vector. Next, following equation (3.19) we could obtain $\mathbb{P}(outage)$. After that, I will uncondition the user locations by averaging over those 10000 user locations vector. In this way I can obtain the $E(\mathbb{P})$ for one candidate antenna locations vector $\boldsymbol{L}$. And after repeating the above steps and obtaining 188 values of $E(\mathbb{P})$, I will choose the one with minimum value and the corresponding antenna locations vector $\boldsymbol{L}$ will be our optimum antenna layout $\boldsymbol{L}'$.

Comparing to numerical computation, simulation is a more feasible method since it's much faster. Optimum antenna layout can be achieved in just several hours using simulation.

For the simulation, antenna's height $\hbar$ is assumed a value of 0.05, R is assumed a value of 1 bits/sec/Hz, η is assumed a value of 4, and M=4. These parameters are chosen the same as in the numerical computation.

3.6.2 Optimum antenna layout for M=4

In this section, we will show the simulation result of optimum antenna layout for circular symmetric antenna layout with M=4.

From simulation results, we find that the optimal radius of the antenna circle is 0.55, which results in the minimum expected value of outage probability of $E(\mathbb{P}) = 0.009$. Comparing to the case that all the antennas are at the center, the optimal location provides almost 40% improvements in system's average outage probability. Fig. 3.4 shows the $E(\mathbb{P})$ for 4 antennas as a function of the first antenna's location $(L_1, \Theta_1, \hbar)$. Different curves representing different angle Θ_1. We can see the value of Θ_1 has minor impact on $E(\mathbb{P})$ and that's why we only show the optimum radius. Also, we can tell that the optimum antenna layouts obtained through simulation and numerical computations are similar. (in numerical results, the minimum average uplink outage probability of the DAS has the value of 0.0087 when the radius of antennas circle is 0.58.)

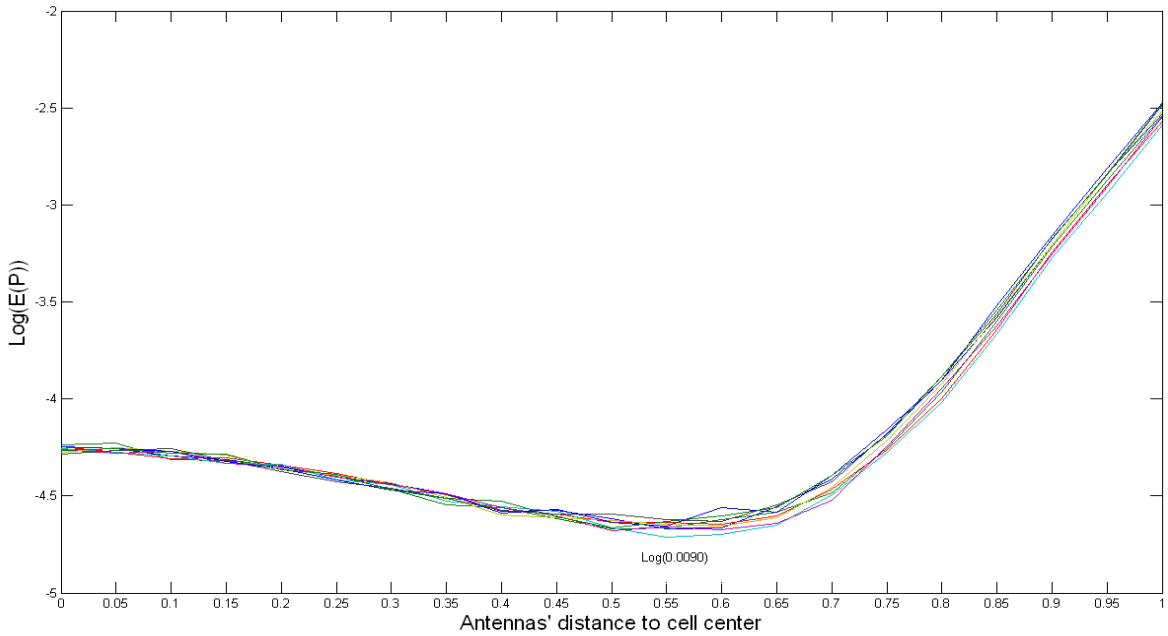

Fig. 3.4: Simulation result for system's average outage probability for 4 antennas as a function of the first antenna's location.

3.6.3 Worst Case for *M*=4

In this section, we are going to present the simulation result for the worst case in Fig 3.5. This is not for minimizing system's average outage probability $E(\mathbb{P})$, but for minimizing $\mathbb{P}(outage)$ when the co-channel interferences are the most severe, which means that the neighboring users are at the closet locations towards the target cell.

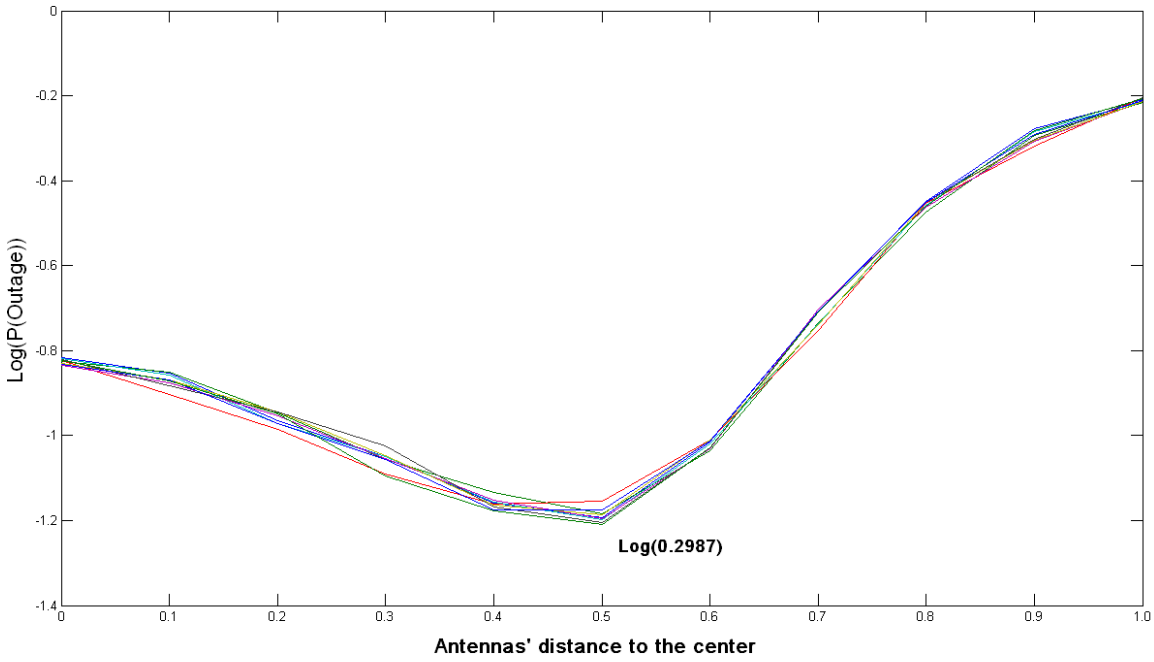

Fig. 3.5: Simulation result for outage probability for 4 antennas as a function of the first antenna's location in the worst case.

From Fig. 3.5, we can see that when antennas' distances to the center are 0.5, the outage probability is minimized at 0.2987. This is 33 times worse than the optimized average outage probability of the system.

3.6.4 1, 5 antennas

In this section, we are going to present the optimum results for the average case together with the worst case for M=1, 5.

3.6.4.1 *M*=1

A. For the system' average outage probability $E(\mathbb{P})$

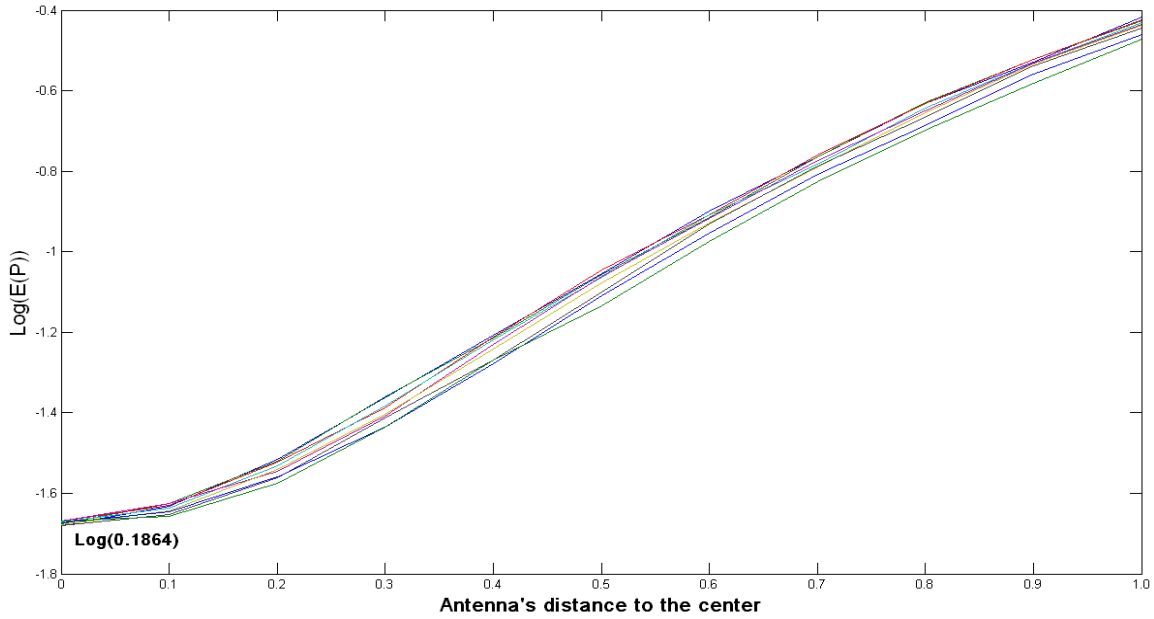

Fig. 3.6 a: Simulation result for system's average outage probability for 1 antenna as a function of the first antenna's location

B. For the worst case outage probability $\mathbb{P}(outage)$

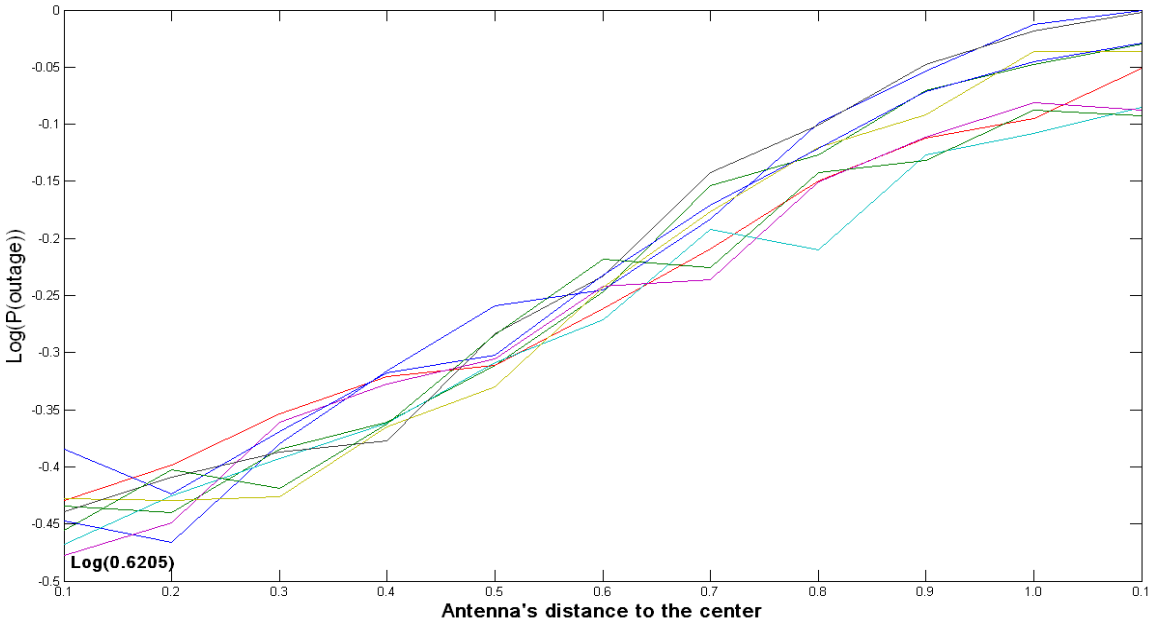

Fig. 3.6 b: Simulation result for outage probability for 1antenna as a function of the first antenna's location in the worst case.

3.6.4.2 *M*=5

A. For the system' average outage probability $E(\mathbb{P})$

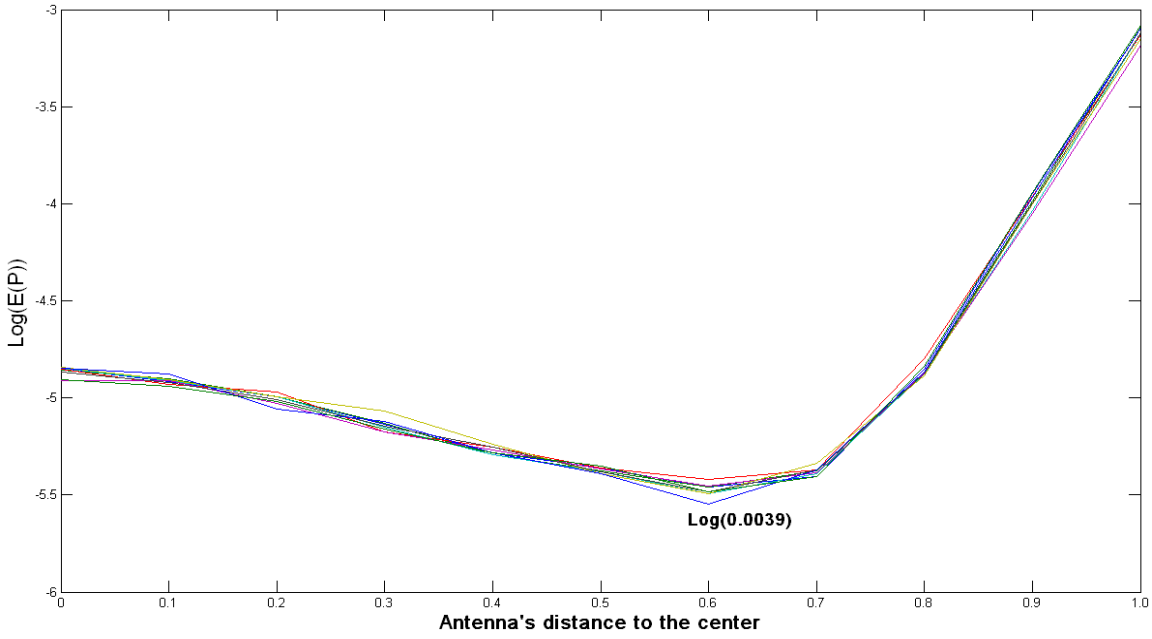

Fig. 3.7 a: Simulation result for system's average outage probability for 5 antennas as a function of the first antenna's location

B. For the worst case's outage probability $\mathbb{P}(outage)$

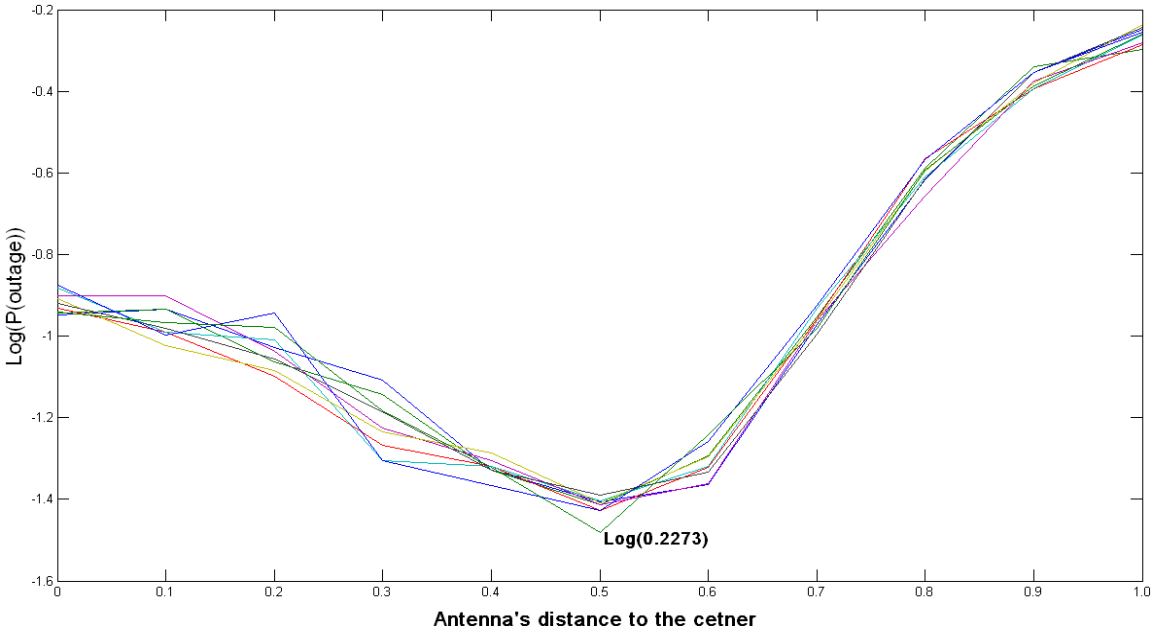

Fig. 3.7 b: Simulation result for outage probability for 5 antennas as a function of the first antenna's location in the worst case.

3.6.5 Summaries

In this section, we are going to give summaries of the simulation results for different value of M .

A. For minimizing system' average outage probability $E(\mathbb{P})$

	1 antenna	2 antennas	3 antennas	4 antennas	5 antennas
Average outage probability $E(\mathbb{P})$	0.1864	0.0633	0.0233	0.0090	0.0039
Antenna's optimum distance to the center	0	0.2	0.5	0.55	0.6
Improvements of deploying one more antenna	0	0.1231	0.04	0.014	0.0054
Improvements in percentage	0	66%	63%	61%	57%

Table 3.3: Optimum radius of antenna circle for minimizing E($\mathbb{P}$)

B. For minimizing $\mathbb{P}(outage)$ in the worst case

	1 antenna	2 antennas	3 antennas	4 antennas	5 antennas
$\mathbb{P}(outage)$ in the worst case	0.6205	0.4841	0.3629	0.2987	0.2273
Antenna's optimum distance to the center	0	0.3	0.5	0.5	0.5
Improvements of deploying one more antenna	0	0.1364	0.1312	0.0542	0.0714
Improvements in percentage	0	22%	23%	15%	24%

Table 3.4: Optimum radius of antenna circle for minimizing $\mathbb{P}(outage)$ in the worst case

From Table 3.3, we can see that for $E(\mathbb{P})$, a new antenna will bring improve 62% in performance. And as the amount of antenna increases, the radius of antenna circle

asymptotically reaches 0.6. We did not present the angle of the antenna's location in the above table since figures above show that angles have minor influence on the optimum locations of antennas.

From Table 3.4, we can see that for minimizing $\mathbb{P}(outage)$ in the worst case, a new antenna will improve about 20% in performance. From Figs. 3.5 to 3.7, we can see though the angles do influence the outage probability $\mathbb{P}(outage)$, as *M* rises, the impact of it is reducing, and when *M*=5, the influence is very little, as shown in Fig. 3.7. So no information of angle is presented here either.

The above two tables are summarizes of the simulation results. The results are based on our earlier assumptions that the antennas are symmetrically distributed on a circle centered at the center of the cell, and radius of each cell has the unitary value of 1. The antenna's height $\hbar$ has value of 0.05, the path-loss exponent $\eta = 4$, and the required transmission rate *R*=1 bit/Hz/Sec. Explicitly, a higher *R* will result in higher outage probability and vice the verse.

At this point, we have obtained the optimum antenna layout through numerical computations and simulations. We have tried to obtain the optimum placements of antennas for minimizing system's average uplink outage probability by making several reasonable assumptions for simplification: 1. There is no source of noise other than co-channel interferences; 2. The antennas are symmetrically distributed on a circle

centered at the center of the cell.

From the numerical and simulation results, we can tell that the optimum antenna layout is depending on the amount of antennas, and the optimal locations of the antennas are not at the cell center except for the 1 antenna case. Also, radius of antennas circle dominates the outage probability, while the corresponding angles influence little. Furthermore, every time one more antenna being deployed, it can improve 62% in the system's average outage probability $E(\mathbb{P})$, and about 20% improvements to $\mathbb{P}(outage)$ in the worst case whereas the antenna circle expands as the amount of antennas increases in both average and worst case.

Also, we notice that $E(\mathbb{P})$ in this chapter are relatively smaller than the outage probability p we have been using in studying the queuing delay violation probability in Chapter 2 with the value $p = 0.1$, the reason for that is in Chapter 3 we have chosen R the required transmission rate of a user, to be a small value of R=1 bit/Hz/Sec. However, when R increases, $\mathrm{E}(\mathbb{P})$ will increase for sure. For example, when R=2 bit/Hz/Sec, the minimum value of system's outage probability achieves 0.067 when the radius of antennas circle has the value of 0.5. This is obtained through simulation.

Chapter 4. Conclusion and future work

Presently, distributed broadband wireless communication (BWC) system is a very promising wireless technology due to its low cost and high performance. It contains a distributed antenna system (DAS) connected to a base station with optical fiber. This thesis determines the queuing delay violation probability for a multi-priority queue under heavy traffic load as a function of the outage probability of the DAS. The relation between these two QoS metrics is presented. And we have also studied the optimum antenna layout that minimizes the antenna outage probability.

In the queuing delay violation probability analysis, an asymptotic method is adopted for calculating the energy functions using the central limit theorem for renewal processes, and an analytical approximation is given to calculate the number of departures of a low priority traffic in the presence of high priority traffics in a certain duration. With the above two steps, we could obtain the queuing delay violation probability for a general multi-priority queue with any number of priority levels and arbitrary renewal arrival/departure process while former works are mostly focusing on single priority queue with constant arrival/departure rate. Numerical results show that the reduction in outage

probability will not only improve the queuing delay but also reduce the packet loss probability; it will also improve the bandwidth and energy efficiencies. Simulation results have been also presented to show accuracy of our analysis.

Since outage probability is a crucial factor in the QoS and performance of DAS, we have investigated the optimum distributed antenna layout that results in the minimum average uplink outage probability. The studied model includes path-loss and Rayleigh fadings, and inter-cell interferences are properly taken into account in our cellular topology. The exact distribution of the system's outage probability with a given set of user locations has been determined and this achievement appears to be the first in the literature. Unfortunately, the closed form expression of the optimum antenna layout could not be obtained due to huge mathematic complexity, even with the simplification that antennas will be symmetrically located on a circle centered at the cell center. Thus, we turn obtain the numerical results of the optimum antenna layout using Robbins-Monro algorithm from stochastic approximation. The results show that for a cell with 4 antennas, the optimum radius of the antenna circle is 0.58 which achieves the minimum outage probability of 0.0087 for R=1 bits/sec/Hz. Simulation results show that deployment of one more antenna can bring almost 62% improvement in the system' average outage probability $E(\mathbb{P})$, and about 20% improvement in the system's outage probability $\mathbb{P}(outage)$ in the worst case whereas the antennas circle expands as the amount of antennas increases in both average and worst case.

Our analysis on the queuing delay violation probability and the optimum antenna layout in DAS will be useful in designing distributed BWC systems and the results are very easy to use. What's more, it should be noted that the analysis of queuing delay violation probability is not just limited to the distributed BWC systems, in fact, it is quite general and it applies to the delay attribute of a multi-priority queue with renewal arrival and departure processes in any kind of communication system.

The following possible future works is envisioned,

1. Derivation of a closed form of the optimum antenna layout, though huge mathematic complexities are involved.

2. Extending the optimum antenna layout study by including power constraints on each user since power consumption is a very important issue, examples might be [9] and [10].

3. Try the analysis of optimum antenna layout based on the combination of DAS and CAS. This combined system model might provide a smooth transition from CAS to the DAS by using existing infrastructures.

4. Verify the discovery from simulation results in [10] that shadowing or multi-path Raleigh fading has no effect on the optimal location of antennas in optimizing

system's capacity. If this conclusion is true, it will help reduce the complexity a lot in dealing with similar problems.

5. While the required transmission rate R of users are different which is exactly what happens in the real world, the optimum antenna layout in minimizing the average uplink outage probability of the system should be a function of the distribution of R. And the work on this problem may have to be depend on either solving problem 1 or 4.

References

[1] Mohr, W. ; Monserrat, J.F. ; Osseiran, A. ; Werner, M. “IMT-ADVANCED AND NEXT-GENERATION MOBILE NETWORKS [Guest Editorial]” in *Communications Magazine, IEEE* Volume : 49 , Issue:2 page(s): 82 – 83, February 2011

[2] Wang, Jiangzhou; Adachi, F.; Gameiro, A.; Gomes, N.J.; Kitayama, K-I.; Monteiro, P.; Sawahashi, M.; Xia, Xiang-Gen “Guest Editorial: Distributed Broadband Wireless Communications” in *Selected Areas in Communications, IEEE Journal on,* Volume: 29 , Issue: 6 Page(s): 1121 – 1122, 2011

[3] Jungwon Lee; Toumpakaris, D.; Wei Yu “Interference Mitigation via joint detection” in *Selected Areas in Communications, IEEE Journal on,* Volume: 29 , Issue: 6 Page(s): 1172 – 1184, 2011

[4] Clark, M.V.; Willis, T.M., III; Greenstein, L.J.; Rustako, A.J., Jr.; Erceg, V.; Roman, R.S. “Distributed Versus Centralized Antenna Arrays in Broadband Wireless Networks” in *VTC 2001 Spring. IEEE VTS 53rd ,* Volume: 1 Page(s): 33 – 37, 2001

[5] Wei Feng; Xibin Xu; Shidong Zhou; Jing Wang; Minghua Xia "Sum Rate Characterization of Distributed Antenna Systems With Circular Antenna Layout" in *Vehicular Technology Conference, 2009. VTC Spring 2009. IEEE 69th* , Page(s): 1 – 5, 2009

[6] Jiansong Gan; Yunzhou Li; Shidong Zhou; Jing Wang "On Sum Rate of Multi-User Distributed Antenna System With Circular Antenna Layout" in *Vehicular Technology Conference, 2007. VTC-2007 Fall. 2007 IEEE 66th* , Page(s): 596 – 600, 2007

[7] Wei Feng; Yunzhou Li; Jiansong Gan; Shidong Zhou; Jing Wang; Minghua Xia "On the Size of Antenna Cluster in Multi-User DAS" in *Communications and Networking in China, 2008. ChinaCom 2008. Third International Conference on* , Page(s): 1101 – 1105, 2008

[8] Hairuo Zhuang; Lin Dai; Liang Xiao; Yan Yao "Spectral efficiency of distributed antenna system with random antenna layout" in *Electronics Letters*, Volume: 39 , Issue: 6 ,Page(s): 495 – 496, 2003

[9] Lin Dai "A Comparative Study on Uplink Sum Capacity with Co-Located and Distributed Antennas" in *Selected Areas in Communications, IEEE Journal on,* Volume: 29 , Issue: 6 ,Page(s): 1200 – 1213, 2011

[10] Firouzabadi, S.; Goldsmith, A.” Optimal Placement of Distributed Antennas in Cellular Systems” in *Signal Processing Advances in Wireless Communications (SPAWC), 2011 IEEE 12th International Workshop on,* Page(s): 461 – 465, 2011

[11]Zennaro, D.; Tomasin, S.; Vangelista, L. “Base Station Selection in Uplink Macro Diversity Cellular Systems with Hybrid ARQ” in *Selected Areas in Communications, IEEE Journal on*, Volume: 29 , Issue: 6 Page(s): 1249 – 1259, 2011

[12]Linnartz, J.-P.M.G. “Exact Analysis of the Outage Probability in Multiple-User Mobile Radios” in *Communications, IEEE Transactions on ,* Volume: 40 , Issue: 1 Page(s): 20 – 23, 1992

[13] Qinghe Du; Xi Zhang “QoS-Aware Base-Station Selections for Distributed MIMO Links in Broadband Wireless Networks” in *Selected Areas in Communications, IEEE Journal on* Volume: 29 , Issue: 6 Page(s): 1123 – 1138, 2011

[14]Alighanbari, A.; Sarris, C.D. “High Order S-MRTD Time-Domain Modeling of Fading Characteristics of Wireless Channels” in *Antennas and Propagation Society International Symposium 2006, IEEE* Page(s): 2165 – 2168, 2006

[15] Bernard Sklar “Digital Communications, Fundamentals and Applications,2nd edition.” Chapter 15 *Prentice Hall PTR* , January 11, 2001

[16] Theodore S. Rappaport "Wireless Communication Principles and Practice. Chapter4" *Prentice Hall PTR,* 1996

[17] Youssef, N.; Kawabata, T. "On the probability density functions of outage and inter-outage durations of the capacity of Rayleigh fading channels" in *Wireless Communications, IEEE Transactions on* , Volume: 8 , Issue: 2 Page(s): 529 – 534 , 2009

[18]Yi Zhao; Adve, R.; Teng Joon Lim "Outage Probability at Arbitrary SNR with Cooperative Diversity Networks" *Communications Letters, IEEE* , Volume: 9 , Issue: 8 Page(s): 700 – 702, 2005

[19] T.M. Cover and J.A.Thomas "Element of Information Theory", John Wiley,1991

[20] Alberto Leon-Garcia "Probability, Statistics and Random Process for Electrical Engineering 3rd edition", Pearson Prentice Hall, 2008

[21]Peter Rabinovitch& Danny De Vleeschauwer "What is EffectiveBandwidth" *http://www3.sympatico.ca/peter.rabinovitch/eb.pdf*

[22] Chen-Shang Chang; Thomas, J.A. "Effective Bandwidth in High-speed Digital Networks" in *Selected Areas in Communications, IEEE Journal on* , Volume: 13 , Issue: 6 Page(s): 1091 – 1100, 1995

[23] Dapeng Wu; Negi, R. “Effective Capacity---A Wireless Link Model for Support of Quality of Service” in *Wireless Communications, IEEE Transactions on ,* Volume: 2 , Issue: 4 Page(s): 630 – 643 , 2003

[24] Xinzheng Wang; Pengcheng Zhu; Ming Chen “Antenna Location Design for Generalized Distributed Antenna Systems” in *IEEE COMMUNICATIONS LETTERS,* VOL. 13, NO. 5, MAY 2009

[25] Yunzhi Qian; Ming Chen; Xinzheng Wang; Pengcheng Zhu “Antenna Location Design for Distributed Antenna Systems with Selective Transmission” in *Wireless Communications & Signal Processing, 2009. WCSP 2009. International Conference on*, 2009

[26] Alan V.Oppenheim, Alan S.Willsky with S.Hamid Nawab “Signals and Systems” second edition, Prentice Hall

[27] International Telecommunication Union “ITU-R M.1645: Framework and overall objectives of the future development of IMT-2000 and systems beyond IMT-2000”

[28] William Feller “An Introduction to Probability Theory and Its Applications, Volume 2”, Chapter Ⅺ,John Wiley & Sons, Inc.

[29] Harold J.Kushner and Dean S.Clark “Stochastic Approximation Methods for Constrained and Unconstrained Systems”, Chapter 1, Spinger-Verlag, New York, Heidelberg, Berlin

[30] B. T. Polyak and A. B. Juditsky “Acceleration of Stochastic Approximation by Averaging” *SIAM J. CONTROL AND OPTIMIZATION Vol. 30, No. 4, pp. 838-855, July 1992*

[31] Ronald Graham, Donald Knuth, and Oren Patashnik “Concrete mathematics (2 ed.)”. p. 446, Addison-Wesley, 1994